View metadata, citation and similar papers at core.ac.uk

brought to you by CORE

provided by Texas A&M Repository

REACTION MECHANISM OF CUMENE HYDROPEROXIDE DECOMPOSITION IN CUMENE AND EVALUATION OF ITS REACTIVITY HAZARDS

A Thesis

by

YUAN LU

Submitted to the Office of Graduate Studies of
Texas A&M University
in partial fulfillment of the requirements for the degree of

MASTER OF SCIENCE

August 2008

Major Subject: Chemical Engineering

REACTION MECHANISM OF CUMENE HYDROPEROXIDE DECOMPOSITION IN CUMENE AND EVALUATION OF ITS REACTIVITY HAZARDS

A Thesis

by

YUAN LU

Submitted to the Office of Graduate Studies of
Texas A&M University
in partial fulfillment of the requirements for the degree of

MASTER OF SCIENCE

Approved by:

Chair of Committee,	M. Sam Mannan
Committee Members,	Rayford Gaines Anthony
	Debjyoti Banerjee
Head of Department,	Michael V Pishko

August 2008

Major Subject: Chemical Engineering

ABSTRACT

Reaction Mechanism of Cumene Hydroperoxide Decomposition in Cumene and Evaluation of Its Reactivity Hazards. (August 2008)

Yuan Lu, B.S., East China University of Science and Technology;

M.S., East China University of Science and Technology

Chair of Advisory Committee: Dr. M. Sam Mannan

Cumene hydroperoxide (CHP), a type of organic peroxide, is widely used in the chemical industry for diverse applications. However, it decomposes and undergoes highly exothermic runaway reactions under high temperature because of its unstable peroxide functional group. The risk of runaway reaction is intensified by the fact that operation temperature of CHP is close to its onset temperature in many cases.

To ensure safe handling of CHP in the chemical industry, a lot of research has been done on it including theoretical research at the microscopic level and experimental research at the macroscopic level. However, the unstable radicals in the CHP decomposition reactions make it difficult to study its reaction pathway, and therefore lead to incomplete understanding of the reaction mechanism. The slow progress in theoretical research hinders the application of the theoretical prediction in experimental research. For experimental research, the lack of integration of operational parameters into the reactivity evaluation limits its application in industrial process.

In this thesis, a systematic methodology is proposed to evaluate the reactivity hazards of CHP. This methodology is a combination of theoretical research using computational quantum chemistry method and experimental research using RSST^{TM}. The theoretical research determined the dominant reaction pathway of CHP decomposition reaction through the study of thermodynamic and kinetic stability, which was applied to the analysis of experimental results. The experimental research investigated the effect of CHP concentration on runaway reactions by analyzing the important parameters including temperature, pressure, self-heat rate and pressure rate. This methodology could also be applied to other organic peroxides or other reactive chemicals.

The results of theoretical research on reaction mechanism show that there is a dominant reaction pathway, which consumes most of the CHP in decomposition reaction. This conclusion agrees with the experimental results that 40 wt% is a critical point for almost all important parameters of runaway reactions. In the high concentration range above 40 wt%, some unknown reaction pathways are involved in decomposition of CHP because of lack of cumene. The shift of reaction mechanism causes the change of the effect of concentration on runaway reactions.

DEDICATION

To my parents: Jian’an Lu and Yuluan Geng

ACKNOWLEDGEMENTS

I would like to express my deep and sincere gratitude to my advisor, Dr. M. Sam Mannan, Director of May Kay O'Connor Process Safety Center (MKOPSC). His wide knowledge and his logical way of thinking have been of great help for me. His guidance and encouraging have provided a good basis for this thesis. Above all and the most needed, he provided me selfless support in various ways in my graduate study. I am indebted to him more than he knows.

My thanks and appreciation goes to the committee members, Dr. Rayford Gaines Anthony and Dr. Debjyoti Banerjee for their efforts, time and advice.

I gratefully acknowledge Dr. Steven Zhang, my team leader, research scientist of MKOPSC, for his advice, supervision, and contribution. His involvement with his originality has triggered and nourished my intellectual maturity that I will benefit from in my future life.

I owe my most sincere gratitude to Dr. William J. Rogers, the research scientist of MKOPSC. I have benefited by advice and guidance from him who also always generously grants me his time and effort.

Many thanks go in particular to Victor Carreto Vazquez. As a senior graduate student majored in the area of reactive chemical, he offered me great help in experiment design and equipment operation, which effectively accelerated the progress of my research.

I gratefully thank my officemates, whom I spend most of my time with. In the past two years, we shared the same stressful but happy time, which make us families. Their care, support and encouragement give me confidence and make me warm even in the toughest day.

Also, many thanks go to all the member of MKOPSC for their help to make this research project reach this final stage.

Last but not least, I am deeply grateful to my parents, who gave me life and dedicate all their love to me. In the past twenty –six years, they have always put education as a first priority in my life and raised me to set high goals for myself. Their selfless love supports me to study abroad and fight against any challenge in front me, trying to honor them and myself. They are my everything.

NOMENCLATURE

Symbols	Definition
Subscripts	
adj	Adjusted value
c	Test cell
s	Sample
on	Refer to the onset temperature of a runaway reaction
max	Maximum
meas	Measured value
ϕ	Thermal inertia
δ	Standard deviation
idg	Ideal state
mix	Refer to the effect of mixing
press	Refer to the effect of pressure
vap	Refer to vaporization
Parameters	
A	Frequency factor
E_a	Activation energy
k	Reaction coefficient
$E_a^{\,0}$	Intrinsic barrier
γ_p	Transfer coefficient

C_s	Heat capacity of the sample
C_c	Heat capacity of the test cell
dT/dt	Heat rate
dP/dt	Pressure rate
P	Pressure
T	Temperature
m	Mass
T_{SADT}	Self-accelerating decomposition temperature

Abbreviations

CHP	Cumene hydroperoxide
RSST	Reactive System Screening Tool
ARC	Accelerating Rate Calorimeter
APTAC	Automatic Pressure Tracking Adiabatic Calorimeter
VSP	Vent Sizing Package
AM1	Austin model 1
HF	Hartree-Fock method
DFT	Density Functional Theory method
CBS	Complete Basis Set method
TAM	Thermal Activity Monitor
DIERS	Design Institute for Emergency Relief System
GC	Gas Chromatography
HPLC	High Performance Liquid Chromatography

IR	Infrared Spectroscopy
MS	Mass Spectrometer
TSS	Thermal Safety Software

TABLE OF CONTENTS

LIST OF FIGURES

Page

LIST OF TABLES

Page

CHAPTER I

INTRODUCTION

1.1 Background

Organic peroxides are a group of organic compounds containing the peroxide functional group (ROOR'). The O-O bond in the peroxide functional group of organic peroxides can be easily broken and form free radicals in the form of RO·, which are able to initiate radical reactions. Because of this property, organic peroxides are used worldwide as initiators and catalysts for many polymerization reactions in the polymer, polyester and rubber industries. They are also widely used as accelerators, activators, cross-linking agents, curing and vulcanization agents, hardeners and promoters in the chemical industry. However, the unstable peroxide functional group also makes organic peroxides hazardous materials in the process of production, storage and transportation. Improper operation or management of these processes may trigger runaway reactions of organic peroxides. The runaway reactions can cause dramatic increases of temperature and pressure, therefore leading to various consequences such as tank rupture, fire and explosion. According to the CSB database, out of a total of 167 serious incidents that happened between 1980 and 2001, there were 11 incidents caused by organic peroxides.[1] Because of their wide applications and frequent occurrence of related incidents, research on organic peroxides is becoming an urgent need to ensure its safety in chemical industry.

This thesis follows the style of *Journal of Chemical Information and Computer Science*.

Cumene hydroperoxide (Figure 1) is a typical example of organic peroxide. It is produced via the oxidation of cumene with air in the presence of aqueous sodium carbonate as the catalyst (Figure 2). CHP is primarily used in the production of acetone and phenol. It is also used as a catalyst for rapid polymerization, especially in redox systems, a curing agent for unsaturated polyester resins, an initiator for polymerization of styrene and acrylic monomer, and a chemical intermediate for the cross-linking agent. Commercial CHP is available in the form of CHP/cumene mixture. In this thesis CHP solution refers to the CHP/cumene mixture unless specified otherwise, and wt % means the weight fraction of CHP in solution.

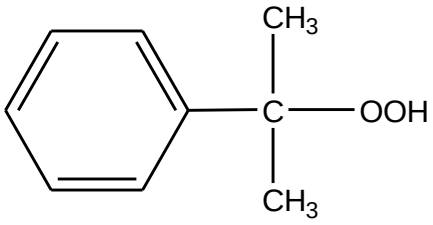

Figure 1 Molecular structure of cumene hydroperoxide

In United States, there are thirteen companies producing CHP, and in 1985, about 1.1 million pounds of CHP were produced in the United States. Approximately 7 billion pounds of CHP are consumed yearly in the United States, indicating that the majority of the CHP needs to be imported.[2]

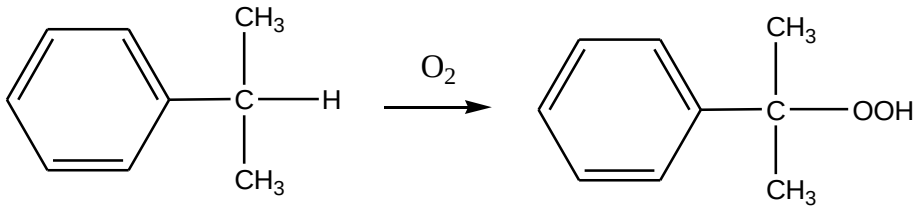

Figure 2 The reaction to produce cumene hydroperoxide

CHP is a colorless to pale yellow liquid with a sharp, irritating odor. It is slightly soluble in water but readily soluble in organic solvents like alcohol, esters, acetone, hydrocarbons, etc. It sinks in water because its density is greater than water. CHP boils at 153 ℃ and its boiling point can be reduced to 100 ℃ under the pressure of 8 mmHg.[3] The major physical-chemical properties of CHP are listed in Table 1.[2]

Table 1 Physical-chemical properties of cumene hydroperoxide

Property	Information	Reference
Physical state	Colorless to pale yellow liquid	Lewis (1993)
Odor	Sharp, aromatic	Radian Corporation (1991)
pH	~ 4	Radian Corporation (1991)
Melting point	< -40°C	Radian Corporation (1991)
Boiling point	153°C 100-101°C @ 8 mmHg	Radian Corporation (1991)

Table 1 continued

Property	Information	Reference
Freezing point	-9°C	Radian Corporation (1991)
Density	1.024 g/mL@ 20°C 1.03 g/mL @ 25°C	Radian Corporation (1991)
Vapor pressure	0.24 mm Hg@ 20°C	HSDB (1997)
Specific gravity	1.05 units	HSDB (1997)
%Volatile (by volume)	100%	Radian Corporation (1991)
Flash point	175°C	HSDB (1997)
Flammability	0.9-6.5%	HSDB (1997)
Heat of combustion	-7400 cal/g	HSDB (1997)
Heat of decomposition	-475 cal/g	HSDB (1997)
Liquid surface tension	25 dynes/cm @ 25°C	HSDB (1997)
Liquid/water interfacial tension	30 dynes/cm @ 25°C	HSDB (1997)
Refractive index	1.5210 @ 20 °C	Aldrich (1996-1997)
Solubility (18 °C)	water: <0.1 mg/mL 95% ethanol: > 100 mg/mL acetone: > 100 mg/mL	Radian Corporation (1991)
Corrosion	Reactive with metal-containing materials	Lewis (1993)

Because of the properties mentioned above, CHP is a hazardous material for production, storage and transportation processes. First, it is flammable. The National Fire Protection Association classified CHP as a class III type flammable.[4] Once it is on fire, phenol

vapor may form from hot material and the burning rate becomes more rapid as fire burns. Second, it is explosive. The explosive vapor/air mixture can be formed if the environmental temperature exceeds 79 °C.[5] Third, it is toxic. Inhalation of CHP vapor can cause headache and burning throat. Liquid CHP may cause severe irritation, burning or even throbbing sensation if it contacts with eyes or skin. Ingestion of CHP may lead to irritation of mouth and stomach.[2]

The biggest hazard of CHP is its reactivity. Basically, CHP is intrinsically unstable and reactive due to its relatively weak –O–O– linkage in the peroxide functional group. The bond-dissociation energy of this linkage is about 20-50 kcal/mol.[6] This functional group is sensitive to heat and incompatible with various contaminants such as bases, acids and metal ions.[7] The breakage of the weak bond can cause the exothermic decomposition of CHP and leads to runaway reactions if the heat generated cannot be removed in time.

CHP is particularly dangerous in chemical processes, where, in many cases, operation temperature is close to the onset temperature of CHP solution. For example, CHP production reactors operate at a temperature range of 115-120°C, while onset temperature for 35 wt% CHP solution (concentration of CHP in reactor) measured by different calorimeters is in the range between 101 and 135°C.[8, 9] For condensation section, which is used to concentrate CHP solution up to 80 wt%, the operation temperature needs to be maintained above the boiling point of 100-101°C under the pressure of 8mmHg, which is close to the onset temperature of CHP solution in this

section.[10] Runaway reactions can occur in various units like oxidation reactors, vacuum condensation units, storage tanks, etc. Severe fires and explosions caused by thermal instability and reactive incompatibility of CHP during transportation, storage, or processing have been reported.[10-13] Therefore, it is of great importance to predict the conditions that might lead to runaway reactions in such processes and assess their consequences. The evaluation results can be used to prevent runaway reactions as well as carry out proper measurements to quench them. The results can also be introduced into the design of related equipments to mitigate consequences of runaway reactions.

A series of codes have been developed exclusively to secure the safety of organic peroxides or CHP in industry. The United Nations suggested that an organic peroxide supplier must make a precise test of self-accelerating decomposition temperature (T_{SADT}) in any specific commercial package.[14, 15] The National Fire Protection Association classified CHP as a class III type flammable.[4] The members of Design Institute for Emergency Relief System (DIERS) emphasized research on the characteristics of pressure relief for organic peroxides.[16]

1.2 Motivation

Compared with its wide application and potential hazards, the research done on CHP is inadequate. Until now, research done on CHP has mainly focused on two areas: theoretical research on CHP decomposition reaction mechanism and evaluation of its reactivity hazards. In theoretical research, decomposition reaction mechanisms were postulated based on the analysis of residuals of CHP decomposition reaction.[10, 17] This

work is based on the assumption that each elementary reaction in the reaction mechanism is thermodynamically feasible. Therefore, without further research on thermodynamic and kinetic stability of CHP reaction mechanism, it is difficult to draw any useful conclusion from the reaction mechanism. The poor understanding of the reaction mechanism also obstructs the application of theoretical research at the microscopic level to experimental research at the macroscopic level.

In the research of reactivity hazard evaluation, experiments have been done to study the kinetics of the CHP decomposition reaction; obtain important thermodynamic and kinetic parameters; research the incompatibility of CHP with contaminants. However, the operation parameters of industrial processes, which determine the potential hazards in process, have rarely been focused in former research. For CHP concentration, a critical operation parameter varying greatly in many processes, its effect on the runaway reactions has only been simply studied in a narrow concentration range (12-35 wt%).[9] It is known that CHP concentration might change the onset temperature of runaway reactions and is able to influence its exothermic behavior.[9, 10] However, lack of systematic research blocks the way to comprehensive understanding of the effect of CHP concentration and integration of its effect into process safety.

In order to effectively evaluate the reactivity hazards and integrate the results into safety issues, further research in the two areas mentioned above are necessary to overcome the existing limitations. In addition, by identification of the interconnections between the

microscopic and macroscopic levels, learning from one level can be applied to the other level to facilitate the research.

1.3 Objective

The first objective of this research is to develop a comprehensive and fundamental understanding of CHP decomposition reaction mechanism. This understanding should include the thermodynamic and kinetic stability of the reaction mechanism. The second objective is to integrate operation parameters into the evaluation of reactivity hazards of CHP. In this research, CHP concentration was chosen to be integrated into the hazards evaluation as it varies frequently in various processes. The third objective is to determine the interconnections between the theoretical research and experimental research. Guided by learning from theoretical research, experimental research can be more efficient and effective.

1.4 Description of the thesis

Chapter II summarizes the previous research performed on CHP and its safety issues.

Chapter III introduces the methodology used in this research. This methodology combines the research conducted at microscopic and macroscopic levels, with interconnections between each other. The research at the microscopic level is implemented using quantum chemistry computation. Experimental thermal analysis is applied in the research at the macroscopic level.

Chapter IV shows the work performed at the microscopic level using quantum chemistry computation with Gaussian 03. Based on the thermodynamic parameters calculated for different levels of quantum chemistry computation, research was conducted to study the thermodynamic and kinetic stability of the reaction mechanism. A dominant reaction pathway was determined according to the results of the reaction mechanism analysis.

Chapter V presents the research on concentration of CHP, an important factor which is able to affect the onset temperature as well as exothermic behavior of runaway reactions. Calorimeter tests were conducted to determine the effect of CHP concentration on runaway reactions. An important conclusion was reached by applying stoichiometry of the dominant reaction pathway to experimental thermal analysis.

Chapter VI is the conclusion for the whole research work of this thesis.

Chapter VII is the recommendation for the future work in this area.

CHAPTER II

LITERATURE REVIEW

Study on the mechanism of CHP decomposition reaction has been performed in the past in various solvents such as saturated hydrocarbons, tertiary alcohols, olefins and organic acids.[9, 17, 18] The reaction mechanisms can be classified into two categories according to properties of solvents: induced decomposition and non-induced decomposition. For the decomposition reactions occurring in cumene, it is believed to be non-induced decomposition reaction and a reaction mechanism was proposed by Kharasch[17]. The decomposition reactions in cumene also were studied experimentally using Gas Chromatography (GC) and High Performance Liquid Chromatography (HPLC). According to the final products determined by analysis, another reaction scheme for thermal decomposition was recommended (Figure 3).[10]

$$2C_6H_5C(CH_3)_2OOH \leftrightarrow [C_6H_5C(CH_3)_2OOH]_2$$
$$C_6H_5C(CH_3)_2OOH \rightarrow C_6H_5C(CH_3)_2O\bullet + \bullet OH$$
$$C_6H_5C(CH_3)_2O\bullet \rightarrow C_6H_5COCH_3 + \bullet CH_3$$
$$C_6H_5C(CH_3)_2H + \bullet CH_3 \rightarrow CH_4 + C_6H_5C(CH_3)_2\bullet$$
$$C_6H_5C(CH_3)_2H + \bullet OH \rightarrow H_2O + C_6H_5C(CH_3)_2\bullet$$
$$C_6H_5C(CH_3)_2O\bullet + C_6H_5C(CH_3)_2H \rightarrow C_6H_5C(CH_3)_2OH + C_6H_5C(CH_3)_2\bullet$$
$$C_6H_5C(CH_3)_2O\bullet + \bullet OH \rightarrow C_6H_5OH + CH_3COCH_3$$
$$C_6H_5C(CH_3)_2\bullet + \bullet OH \rightarrow C_6H_5CH_3C=CH_2 + H_2O$$
$$2C_6H_5C(CH_3)_2\bullet \rightarrow [C_6H_5C(CH_3)_2]_2$$

Figure 3 Scheme 1 for CHP decomposition reaction in cumene

Further research was done to study kinetics of CHP decomposition reaction using different kinds of calorimeters. With the result of isothermal experiments done using Differential Scanning Calorimeter (DSC) under different concentrations and temperatures, the overall order of CHP decomposition was determined to be a constant value of 0.5, which agrees with that obtained through non-isothermal experiment.[10] By using non-isothermal experiments performed in Accelerating Rate Calorimeter (ARC), it was verified that concentration of CHP does not change the value of A ($5.2\pm1.9\times10^{12}$ $min^{-1}M^{1/2}$) and E_a (118.2±1.2 kJ/mol) of decomposition reaction, and therefore has no effect on decomposition reaction rate coefficient k.[9]

The reactivity hazards of CHP are basically related to process temperature as well as concentration. The thermal hazards of CHP decomposition in cumene were evaluated by different calorimeters. Isothermal aging tests for 80 wt% CHP solution carried out by Thermal Activity Monitor (TAM) revealed that exothermic behavior can be detected even under low temperature and it becomes stronger with increased temperature.[19] In these tests, onset temperature of CHP decomposition in cumene was measured as low as 75°C. The overall time of the decomposition reaction varies from 10 days to 43 days for individual experiment. Heat of reaction was determined to be about 1,200±50 J/g for 80 wt% CHP solution.[19] Concentration also was proven to be an important factor for CHP safety issues by tests carried out using ARC[9]. With increased CHP concentration, the decomposition reaction showed stronger exothermic behavior with higher maximum temperature, higher maximum pressure, higher self-heat rate and higher pressure rate. In

the tests, adverse relationship was observed between onset temperature and CHP concentration within a certain range (12-35 wt%): onset temperature decreased with the increase of CHP concentration.[9] However, this tendency could not be repeated in tests carried out by DSC in CHP solution within concentration range of 35-80 wt%.[10] Infrared Spectra was introduced to investigate the CHP decomposition at the atomic level. It was concluded from infrared absorption spectrum that absorption peak of –O-H stretching is shifted with increased CHP concentration. This phenomenon is due to hydrogen-bounded association formed between the –O-O-H functional group and the oxygen atom of the cyclic dimer (Figure 4). As the dimeric associate of CHP is much more stable than its monomer, dimerization reaction of CHP is supposed to be able to affect rate-determining step of CHP decomposition reaction.[10] In order to apply experimental research results to the safety of production, transportation and storage processes of CHP, the critical runaway temperature and unstable reaction criterion, with the initial CHP concentration of 15 wt% and 20 wt%, were evaluated from kinetic parameters of the decomposition reaction. [20]

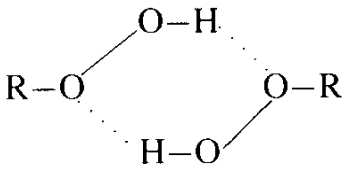

Figure 4 Molecular structure of cyclic dimer

CHP is incompatible with several kinds of contaminants such as bases, acids and metal ions. The runaway reactions caused by contaminants are usually complicated because of complex reaction mechanisms. To investigate the effects of contaminants on CHP runaway reactions, experiments were carried out using DSC in presence of alkalis, acids and ferric ion. The result of the experiments showed that all these contaminants have an effect on the thermal decomposition reaction of CHP. These impurities can effectively lower the onset temperature of runaway reactions by more than 40 °C.[6] The maximum onset temperature reduction occurs when CHP is mixed with ferric ion, as the onset temperature was reduced from 135 °C to 40 °C.[6] Among these three contaminants, alkalis and ferric ion were found to be more effective to intensify the exothermic behavior of runaway reactions, with more than 25 % additional heat generation detected by thermograph according to empirical data. Also, alkalis and ferric ion were found to be positive for heat generation of the decomposition reactions and the peak power at lower temperature, which makes CHP more unstable and hazardous. Further research was done in Vent Sizing Package (VSP) using adiabatic mode to quantify the effect of these contaminants. The experimental data revealed that in presence of only 1 wt% of impurities, the onset temperature of CHP was obviously lower than that of pure CHP. Mixing CHP solution with alkalis can greatly intensify the exothermic behavior of the decomposition reactions, with unusually high self-heat rate, maximum temperature and maximum pressure. However, concluded from experimental data, acids and ferric ion were found be little effective on thermal parameters except onset temperature. Considering the difference of performance of these contaminants, it was postulated that

the mechanisms of runaway reactions initiated by these additives should be significantly different and the speculated decomposition mechanisms in presence of each contaminant are shown in Figures 5, 6 and 7.[7]

$$NaOH + C_6H_5C(CH_3)_2OOH \rightarrow C_6H_5C(CH_3)_2OO^-Na^+ + H_2O$$
$$C_6H_5C(CH_3)_2OOH \rightarrow C_6H5(CH_3)_2O\bullet + \bullet OH$$
$$C_6H_5C(CH_3)_2OO^- + C_6H_5C(CH_3)_2H \rightarrow C_6H_5C(CH_3)_2\bullet + C_6H_5C(CH_3)_2O\bullet + OH^-$$
$$C_6H_5C(CH_3)_2O\bullet \rightarrow C_6H_5COCH_3 + \bullet CH_3$$
$$C_6H_5C(CH_3)_2H + \bullet CH_3 \rightarrow CH_4 + C_6H_5C(CH_3)_2\bullet$$
$$C_6H_5C(CH_3)_2O\bullet + C_6H_5C(CH_3)_2H \rightarrow C_6H_5C(CH_3)_2\bullet + C_6H_5C(CH_3)_2OH$$
$$C_6H_5C(CH_3)_2O\bullet + \bullet OH \rightarrow C_6H_5OH + CH_3COCH_3$$
$$C_6H_5C(CH_3)_2\bullet + \bullet OH \rightarrow C_6H_5CH_3 = CH_2 + H_2O$$
$$2C_6H_5C(CH_3)_2\bullet \rightarrow \left[C_6H_5C(CH_3)_2\right]_2$$

Figure 5 Scheme 2 for alkaline CHP decomposition reaction

$$C_6H_5C(CH_3)_2OOH + A \rightarrow [C_6H_5C(CH_3)_2O]^+ + AOH^-$$
$$[C_6H_5C(CH_3)_2O]^+ \rightarrow [C_6H_5O(CH_3)_2C]^+$$
$$C_6H_5C(CH_3)_2OOH + [C_6H_5O(CH_3)_2C]^+ + (CH_3)_2CO + C_6H_5OH$$
$$C_6H_5C(CH_3)_2OOH \rightarrow C_6H_5C(CH_3)_2O\bullet + \bullet OH$$
$$C_6H_5C(CH_3)_2O + C_6H_5C(CH_3)_2H \rightarrow C_6H_5C(CH_3)_2\bullet + C_6H_5C(CH_3)_2OH$$
$$C_6H_5C(CH_3)_2\bullet + \bullet OH \rightarrow C_6H_5CH_3 = CH_2 + H_2O$$
$$C_6H_5C(CH_3)_2OH + A \rightarrow C_6H_5C(CH_3)_2^+ + B + H_2O$$
$$C_6H_5C(CH_3)_2^+ + B \rightarrow C_6H_5(CH_3)C = CH_2 + A$$
$$2C_6H_5C(CH_3)_2OOH \rightarrow 2C_6H_5C(CH_3)_2O\bullet + H_2O_2$$
$$C_6H_5C(CH_3)_2^+ + H_2O_2 + B \rightarrow C_6H_5C(CH_3)_2OOH + A$$
$$C_6H_5C(CH_3)_2^+ + C_6H_5(CH_3)_2C = CH_2 + B \rightarrow \dim er + A$$

Figure 6 Scheme 3 for acidic CHP decomposition reaction

$$Fe^{3+} + C_6H_5C(CH_3)_2OOH \rightarrow Fe^{2+} + C_6H_5C(CH_3)_2OO\bullet + H^+$$
$$C_6H_5C(CH_3)_2OO\bullet + C_6H_5C(CH_3)_2H \rightarrow C_6H_5C(CH_3)_2OOH + C_6H_5C(CH_3)_2\bullet$$
$$C_6H_5C(CH_3)_2OOH + H^+ \rightarrow [C_6H_5C(CH_3)_2O]^+ + H_2O$$
$$[C_6H_5C(CH_3)_2O]^+ \rightarrow [C_6H_5O(CH_3)_2C]^+$$
$$C_6H_5C(CH_3)_2OOH + [C_6H_5O(CH_3)_2C]^+ \rightarrow [C_6H_5C(CH_3)_2O]^+ + (CH_3)_2CO + C_6H_5OH$$
$$C_6H_5C(CH_3)_2OOH \rightarrow C_6H_5C(CH_3)_2O\bullet + \bullet OH$$
$$C_6H_5C(CH_3)_2O\bullet + C_6H_5C(CH_3)_2H \rightarrow C_6H_5C(CH_3)_2\bullet + C_6H_5C(CH_3)_2OH$$
$$C_6H_5C(CH_3)_2\bullet + \bullet OH \rightarrow C_6H_5CH_3C = CH_2 + H_2O$$

Figure 7 Scheme 4 for ion-induced CHP decomposition reaction

In another research, detailed work was done to study incompatible characteristics of CHP mixed with alkaline solution utilizing DSC.[6] By mixing with different kinds of alkaline solutions, CHP was found to be more unstable because of lower onset temperature, with the greatest reduction of 60 °C. The great reduction of onset

temperature indicated that hydroxide ion is able to trigger runaway reactions at lower temperature. The dosing ratio and the concentration of alkaline solution were also believed to be important factors for the CHP runaway reactions. According to the exothermic profiles recorded by DSC, the heat generation of the decomposition reaction decreased from 1200 to 330 J/g, as dosing ration increased from 20:1 to 1:1 and concentration increased from 1 to 9 N. It was observed from the profiles that small amount of alkalis was able to induce the initial thermal behavior and moderate the main thermal behavior. Further research was done to determine the reaction mechanism of CHP decomposition in presence of sodium hydroxide. Using Gas Chromatography (GC)/ mass spectrometer (MS) and Infrared spectroscopy (IR) to determine the residuals after the decomposition reaction, a reaction mechanism was recommended which was different with previous one mentioned earlier (Figure 8).[6]

$$C_6H_5C(CH_3)_2OOH + NaOH \rightarrow C_6H_5C(CH_3)_2OO^-Na^+ + H_2O$$
$$C_6H_5C(CH_3)_2OO^- + C_6H_5C(CH_3)_2OOH \rightarrow C_6H_5(CH_3)CO^- + C_6H_5(CH_3)_2COH + O_2$$
$$C_6H_5(CH_3)_2CO^- + C_6H_5C(CH_3)_2OOH \rightarrow CH_3COC_6H_5 + CH_3OH + C_6H_5C(CH_3)_2O\bullet$$
$$C_6H_5(CH_3)_2CO^- + C_6H_5C(CH_3)_2OOH \rightarrow C_6H_5C(CH_3)_2OH + HO(CH_3)C_6H_5C\bullet$$
$$HO(CH_3)C_6H_5C\bullet + C_6H_5C(CH_3)_2OOH \rightarrow CH_3COC_6H_5 + H_2O + C_6H_5C(CH_3)_2O\bullet$$
$$2HO(CH_3)C_6H_5C\bullet \rightarrow CH_3COC_6H_5 + CH_3(C_6H_5)CHOH$$

Figure 8 Scheme 5 for alkaline CHP decomposition reaction

Compared with experimental research, which is expensive and time-consuming, a kinetic model is a relatively inexpensive and efficient tool to predict runaway reactions

and estimate their consequences. Using kinetic and thermodynamic data obtained from DSC experiments, a kinetic model was built to simulate the runaway reactions of 88 wt% CHP solution by thermal safety software (TSS).[21] In this model, CHP decomposition was believed to be an autocatalysis reaction, therefore a typical kinetic model for autocatalysis was utilized.[22, 23] However, this kinetic model did not agree with models used in other literature. In one article, the reaction rate of this thermal decomposition reaction was believed to be proportional to the square root of CHP concentration.[20] In another publication, based on the assumption that the dimer of CHP is much more stable than monomeric CHP, the dimerization reaction can reach equilibrium very quickly. Therefore, the decomposition reaction rate was also found to be linear to the square root of monomeric CHP concentration.[10] Another problem with this model is its inability to predict overpressure when runaway reactions occur. This disadvantage is mainly caused by DSC used in the research, because it cannot measure pressure in process of experiment.

CHAPTER III

METHODOLOGY

3.1 Introduction

Reactive chemicals are of great concern for chemical industry because of their potential hazards. In order to prevent, control or quench these hazards, it is of great importance to introduce reactivity hazards into the development of relative industrial codes, design of equipments and other safety measurements. The assessment of reactivity is usually addressed in a specific case or a specific chemical viewpoint, because the properties of reactive chemicals vary greatly even in the same group and conditions for different processes or units are also quite different.

However, a generalized methodology is still an ultimate goal for the research of reactive chemicals. In order to deal with great differences of reactive chemicals, common principles of chemical reactions and analysis methods should be the basis of this methodology. This methodology should be able to draw a standard procedure for research on reactive chemicals and make it more convenient and efficient.

3.2 Methodology

This methodology is a combination of research at the microscopic level and macroscopic level, with interconnections between them. The flow sheet of this methodology is shown in Figure 9.

The research at microscopic level is based on quantum chemistry method. Utilizing different theory levels of quantum chemistry method, study on thermodynamic and kinetic stability of the reaction mechanism can be carried out. The fundamental and comprehensive understanding of the reaction mechanism can help to predict important parameters of runaway reactions such as gas generation, heat generation of reaction and stoichiometry, which can be applied to experimental research. In order to ensure the accuracy of theoretical postulations, the results of theoretical research on runaway reactions still need to be validated by experimental data.

The research at macroscopic level is the experimental study of reactivity using calorimetry test. Important parameters such as temperature, pressure, self-heat rate, pressure rate and heat generation can be determined by research at this level, which can be applied directly to industrial processes. As an interconnection between these two levels, results of the microscopic level research can be applied to the macroscopic level research to analyze the experimental result.

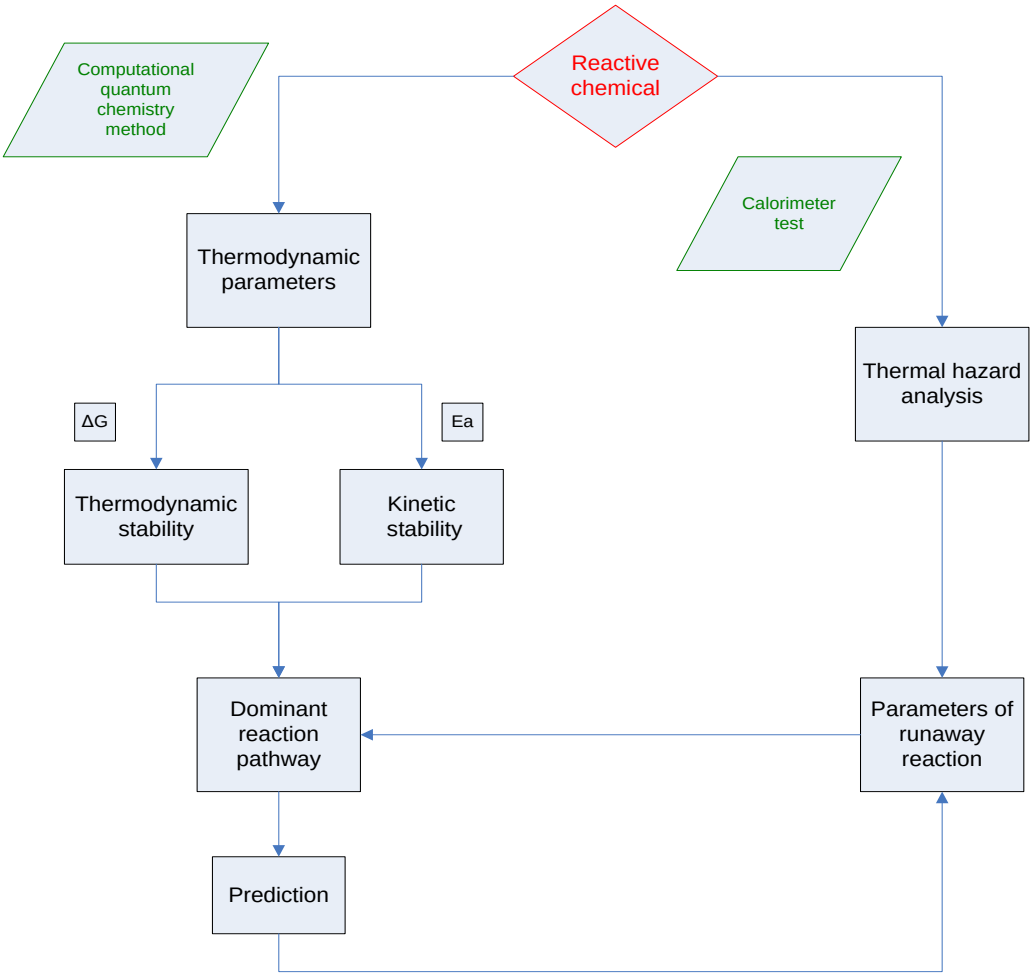

Figure 9 Procedure of methodology

3.3 Theoretical evaluation

3.3.1 Computational quantum chemistry method

Computational quantum chemistry method is based on the quantum molecular theory. The core idea of the theory is that the motion and distribution of electrons can be described in term of probability distributions or molecular orbitals. The method is able to

provide a mathematic description of behavior of electrons, with Schrodinger's equation as its theoretical basis.

A variety of theoretical levels are involved in computational quantum chemistry method. Four different theoretical levels, including semi-empirical method, Hartree-Fock method, Density Functional Theory method and Complete Basis Set method, were selected to perform molecular simulation in this research. The instructions of these theoretical levels are shown as follows.

Semi-empirical method: these methods are based on the Hartree-Fock formalism, but characterized by use of some parameters derived from empirical data. Compared with Hartree-Fock method, some inclusions of electron correlation effect are allowed in semi-empirical method because of using empirical parameters. As such, they are important in dealing with the following tasks or systems where it is too expensive to use full Hartree-Fock method without approximation: very large systems for which semi-empirical method is the only practical quantum chemistry method, the first step for a large system to get a starting structure for a subsequent optimization, ground state molecular systems for which semi-empirical method is well calibrated and well parameterized, obtaining qualitative information about a system such as molecular orbitals, vibrational normal modes or atomic charges. However, application of empirical data also impose this theoretical level a number of limitations: it can only be used for systems where parameters are available for all components atoms; it cannot perform well for hydrogen

bonding, molecule containing poorly parameterized atoms, transition structures, etc. There are a variety of semi-empirical methods, the best known ones among which are AM1, PM3 and MNDO.[24] AM1 is a very common application of the semi-empirical calculations and was utilized in this research.

Hartree-Fock (HF) method: It is an approximate method to determine the ground-state wave function and ground-state energy of a quantum many-body system. This method is based on the assumption that exchange correlation effect between electrons can be ignored due to mean filed approximation. As a good base-level theory, HF method is useful for making initial, first-level prediction for many systems and also good at simulating the structures and vibration frequencies of stable molecules as well as some transition states. However, for some systems where electron correlation is necessary for accurate prediction, HF method is not good enough to do accurate simulation.[24]

Density functional Theory (DFT) method: this method is based on the density functional theory. According to this theory, the ground state energy of a system of electrons is a function of the electron charge density. So, this method calculates the molecular energy using electron density instead of wave functions. In DFT method, the electronic energy is partitioned into several parts and computed separately by functional: kinetic energy, the Coulomb repulsion, electron-nuclear interaction and exchange-correlation term (account for the remainder for the electron-electron interaction). Because of the way to calculate electron correlation, this method can achieve much greater accuracy than HF

method with only relatively low increase in cost.[24] B3LYP is a common theory level of DFT method and was utilized in this research.

Complete Basis Set (CBS) method: this method was developed by George Petersson and other collaborators, trying to deal with the largest errors in *ab initio* calculation resulted from basis set truncation. Typically, in CBS model, the initial calculation starts from frequency calculation and geometry optimization at HF level with a very large basis set. Then the geometry of the molecular is optimized further at MP2 level with a medium-sized basis set, followed by one or more high-level calculations with medium to modest basis sets. CBS method includes a number of methods such as CBS-4, CBS-Q, CBS-APNC, in which CBS-4 method is less expensive.[25-28] CBS-4M is a new version of CBS-4 method. Compared with CBS-4 method, CBS-4M method can reach higher accuracy because of utilizing minimal population localization.[29]

Gaussian 03 is one of the most popular and widely-used computational chemistry package, originally developed by Nobel Prize winner John Pople.[30] It is used by researchers in different areas for research in established and emerging areas of chemical interest.

Starting from the basic laws of quantum mechanics, Gaussian software is able to predict the molecular structures, energies, and vibration frequencies of molecular systems, along with numerous molecular properties derived from the theoretical computations. It is an effective tool to study molecules and reactions, including species and compounds which

are difficult or impossible to be researched experimentally such as short-lived intermediates and transition structures. In this research, all the calculations based on computational quantum chemistry method were performed using this software.

3.3.2 Thermodynamic and kinetic analysis

Reaction mechanism postulated from final products of a reaction gives rise to complex reaction pathways which are hard to be validated. Molecular simulation can be carried out on the reaction mechanism to get preliminary information, based on which further analysis about reaction mechanism can done, such as thermodynamic stability and kinetic stability.

a. Thermodynamic stability

Gibbs free energy change, $\Delta_r G$, can be used to determine the thermodynamic feasibility of chemical reactions. Negative Gibbs free energy change means that the chemical reaction is thermodynamic infeasible, or in another word, this reaction will definitely not take place.[31] Gibbs free energy change can be calculated using the Equation 1.

$$\Delta_r G = \Delta_r H - T\Delta_r S \quad \textbf{(1)}$$

This equation also indicates that Gibbs free energy change is dependent on temperature. So with the increase of temperature, a reaction which was thermodynamically infeasible under a certain temperature might become feasible.

Enthalpy change term, $\Delta_r H$, could be expressed as the sum of four terms contributed by ideal mixture, vaporization, mixture effects (e.g. solvent interaction) and pressure (Equation 2).

$$\Delta_r H = (\Delta_r H^{idg} - \Sigma \nu_i \Delta_{vap} H_i) + \Delta_r H^{mix} + \Delta_r H^{press} \quad \textbf{(2)}$$

$\Delta_r H^{idg}$: enthalpy change of reaction calculated in the ideal gas phase

$\Delta_{vap} H_i$: enthalpies change of vaporization or sublimation evaluated for the N condensed species

$\Delta_r H^{mix}$: effect of mixing and solvent on enthalpy

$\Delta_r H^{press}$: effect of pressure on enthalpy

$\Delta_r H^{idg}$ is defined as the linear combination of enthalpy of formation, given below.

$$\Delta_r H^{idg} = \Sigma \nu_i \Delta_f H^i \quad \textbf{(3)}$$

The entropic change which is involved in Equation 1 could be obtained in a similar way as enthalpy (Equation 4).

$$\Delta_r S = \Delta_r S^{idg} - \sum_{i \in [1...N]} \nu_i \frac{\Delta_{vap} H_i}{T} + \Delta_r S^{mix} + \Delta_r S^{press} \quad \textbf{(4)}$$

$\Delta_r S^{idg}$: entropy change of reaction in ideal gas phase

$\Delta_r S^{mix}$: effect of mixing and solvent on entropy change

$\Delta_r S^{press}$: effect of pressure on entropy change

$\Delta_r S^{idg}$ can be calculated using Equation 5.

$$\Delta_r S^{idg} = \sum_i \nu i S_i^{idg} \quad \textbf{(5)}$$

Usually, the effect of pressure on enthalpy and entropy is much less significant than other contributions, so it is reasonable to neglect it in the calculation of entropy change and enthalpy change.[31] So, based on this assumption, the Gibbs free energy change could be expressed as the sum of two distributions, reaction in ideal gas phase and the effect of solvent and mixing (Equation 6).

$$\Delta_r G = \Delta_r G^{idg} + \Delta_r G^{mix} \quad \textbf{(6)}$$

In most cases, the effect of solvent and mixture interaction on enthalpy and entropy is relatively small compared with the contribution of reaction in ideal gas phase. Unless particularly strong affinities between solvent and solute, the term corresponding to the effect of mixing and solvent can be neglected.[31]

For a reaction composed of a series of elementary reactions, any elementary reaction involved in the reaction mechanism must be thermodynamically feasible. A postulated reaction pathway would be ruled out if any elementary reaction employed in this pathway is thermodynamically infeasible.[32] A screening procedure was proposed by Bruneton et al. to determine the stoichiometry of chemical reactions (Figure 10).[31] Another indicator for reactivity hazards is enthalpy change of chemical reactions. High enthalpy change means more heat generated in reaction while low value presents less heat generation.

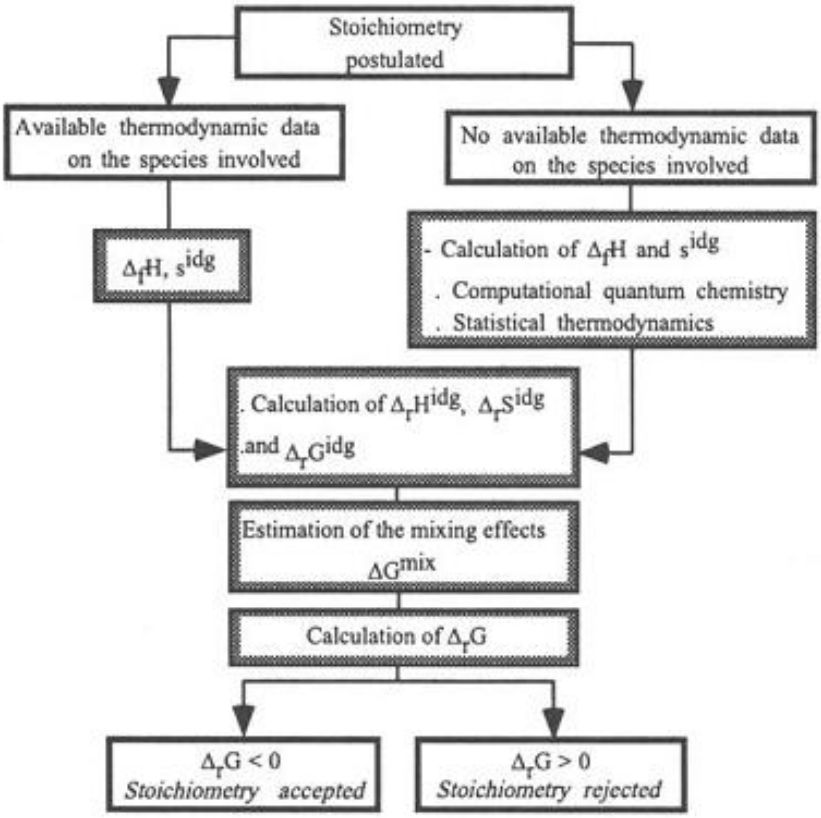

Figure 10 Screening procedure for secondary reaction stoichiometry determination proposed by Bruneton et al. (1997)

b. Kinetic stability

Thermodynamic research is not sufficient to evaluate the reactivity of chemical reactions. A reaction with negative Gibbs free energy still can be immeasurable slow because of the high activation energy. This means the criteria for determining the reactivity of a reaction should include two kinds of stabilities, thermodynamic stability and kinetic stability.

Activation energy is an important parameter to research kinetic stability. Activation energy is defined as the energy that must be overcome by a chemical reaction in order to take place. Arrhenius equation shows the relation between activation energy and the reaction rate (Equation 7):

$$k = A\exp\left(-\frac{E_a}{RT}\right) \quad \textbf{(7)}$$

where k is the rate constant for reaction, A is the frequency factor for reaction, E_a is activation energy, T is temperature of reaction and R is universal gas constant.

Efforts have also been made to find out the relationship between activation energy and measurable parameters. As a meaningful attempt, an equation was developed by Polanyi and Evans, which is also called Polanyi relationship (Equation 8), trying to address such a relationship between activation energy and thermodynamic parameters.

$$E_a = E_a^{\,0} + \gamma_p \Delta H_r \quad \textbf{(8)}$$

where $E_a^{\,0}$ is the intrinsic barrier of reaction, γ_p is the transfer coefficient.

This equation implies that the activation energy varies linearly with the heat of reaction for a series of closely related reactions. Therefore, for the same type of reaction, the activation energy decreases as the reaction becomes more exothermic, indicating the reaction is easier to take place. However, this relationship is imposed with several limitations. One major limitation with Polanyi relationship is that this principle is subjected to small ranges of enthalpy change. Because of this, plot of empirical data over

large range of enthalpy change can not fit Polanyi relationship well. The second limitation is that for very exothermic reaction, the Polanyi relationship may yield unreasonable results such as negative activation energy. Therefore Polanyi relationship is not applicable for strong exothermic reactions.[33]

In order to overcome limitations mentioned above, Marcus developed another relationship for activation energy, which can be viewed as an extension of the Polanyi relationship (Equation 9). This principle is able to address some extreme situations like strong exothermic and strong endothermic reactions.

$$E_a = \left(1 + \frac{\Delta_r H}{4E_a{}^0}\right)^2 E_a{}^0 \qquad \textbf{(9)}$$

Compared with Polanyi relationship, Marcus equation is applicable for some reactions which cannot be addressed by Polanyi relationship. In Marcus equation, activation energy can vary nonlinearly with enthalpy change, which makes this equation fit very well with empirical data in many cases. However, in some other cases, Marcus equation still cannot perform well over a wide range of $\Delta_r H$, which means it can not entirely eliminate the limitation of Polanyi relationship. Another weakness of Marcus equation is that intrinsic barrier is assumed to be a constant, which makes this equation difficult to explain some empirical data.[33]

3.4 Experimental thermal analysis

Calorimeter is the device used for the research of calorimetry. The objective of calorimetry is to study the heat generation of chemical reactions, physical changes as

well as heat capacity. Different kinds of calorimeters have been developed for calorimetry research. The most commonly used calorimeters are Differential Scanning Calorimeter (DSC), Isothermal Microcalorimeter, Accelerated Rate Calorimeters (ARC), etc. In this research, Reactive System Screening Tool was chosen as the equipment to evaluate the reactivity hazards of CHP.

3.4.1 Reactive System Screening Tool

The Reactive System Screening Tool (RSST^{TM}) is a relatively inexpensive calorimeter used to determine the potential hazards quickly and safely in chemical industry. It was developed by Fauske and Associates, Inc. in 1993, with the primary purpose to evaluate emergency relief venting requirements such as gas release rate, energy and effect of two-phase flow. RSST^{TM} can measure and record profiles of temperature and pressure in reaction process, from which other important parameters such as self-heat rate and pressure rate can be derived. The result of RSST^{TM} test can be utilized to research potential runaway reactions as well as corresponding venting size of emergency relief systems. As an economic and effective tool, RSST^{TM} can approach the accuracy of VSP while it still keeps the ease of use of DSC.[34]

The core idea of RSST^{TM} is that the heat loss from the sample is zero if the sample is heated up with sufficient exterior heat even in exothermic process. According to this principle, heat ramp mode is applied in RSST^{TM} by ramping sample at a constant rate through a desired temperature range. Therefore, any deviation from this ramp rate is recognized as the exothermic behavior (Figure 11).[35]

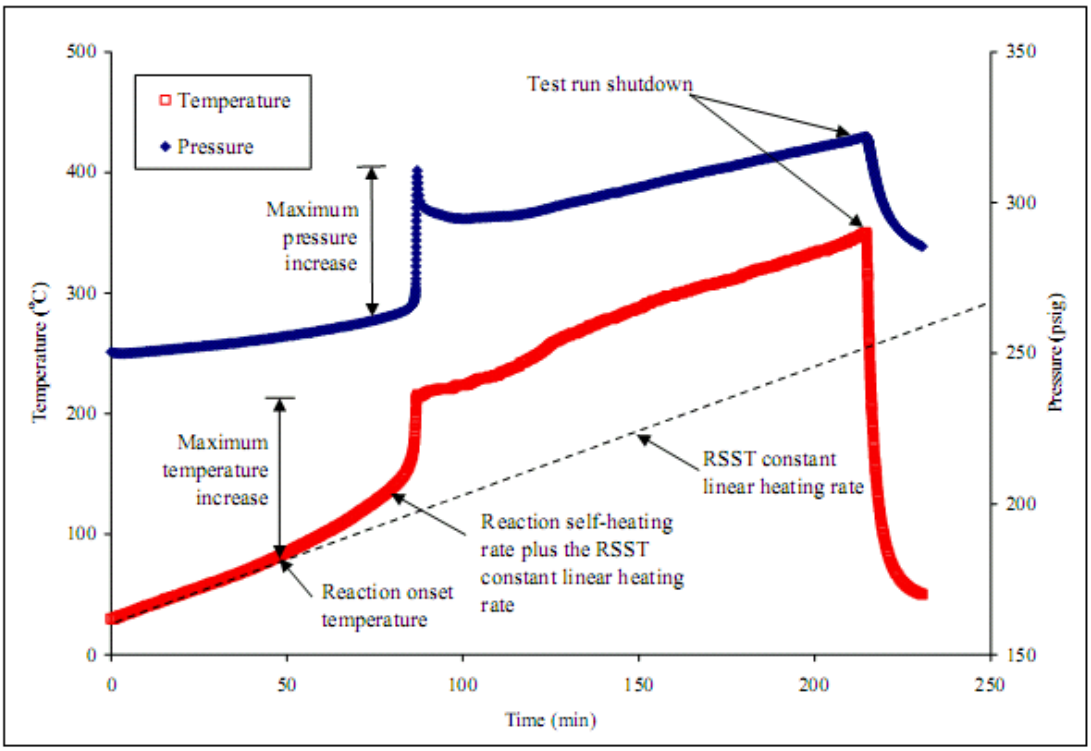

Figure 11 Typical temperature and pressure profiles of RSST™ test

(Adapted from Aldeeb 2003)

3.4.1.1 Equipment description

There are three major components which assemble RSST™: the containment vessel, the control box and the computer control board/software (Figure 12, 14). The containment vessel, which is connected to the control box by wire cable set, houses test cell, thermocouple and insulation assembly. The wire cable set enable the transfer of temperature and pressure singles between control box and sensors, and the power supply

to heater. The control box consists of heater power supply, temperature and pressure signal conditioners, and microprocessor heater controller. The computer board, which is mounted in an expansion board slot of a compatible PC, is also connected to the control box via a wire cable.

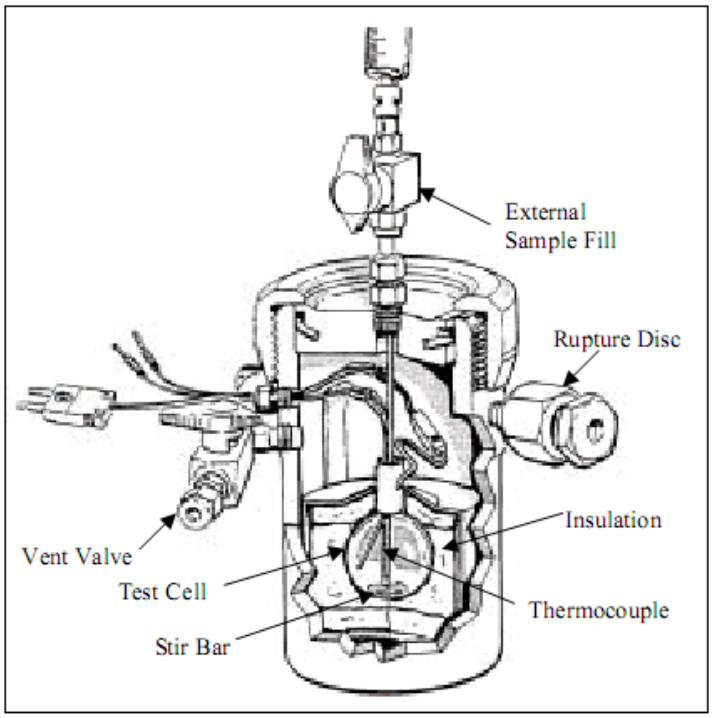

Figure 12 Overall schematic of RSST™ [with permission from Fauske & Associates, Inc.]

The test cell is an open spherical glass cell (10 ml) of low thermal mass placed in a pressure containment vessel (Figure 13). It is well insulated and equipped with either an immersion heater or an external bottom heater. In order to compensate the heat loss and initiate runaway reactions, the heater is controlled by feedback from the sample temperature measurement to overcome heat loss and maintain a fixed temperature ramp

rate. With the computer control option, the imposed ramp rate can be chosen in the range of 0.25 to 2 °C. The software of RSST^{TM} allows the implementation of fixed ramp rate or programmed ramp rate in test procedure. A magnetic stirrer is included in the test cell assembly, driven by magnetic stirrer drive base. The design of open test cell and external filling device makes it possible to add sample during tests.

3.4.1.2 Operation procedure

Before running a test, inspection should be carried out for every main component of RSST^{TM}. Unsuccessful runs might be caused by failure of examining the health of parts exposed to wear and corrosion. The pre-test inspection includes examining on heater, thermocouple, pressure transducer, O-ring, heater/TC penetration gland. Before loading sample, pressure check needs to be done to avoid any potential leak of containment vessel. The calibration check is also necessary to ensure the quality of thermal data, including the calibration check on temperature, pressure and strip chart recorder.

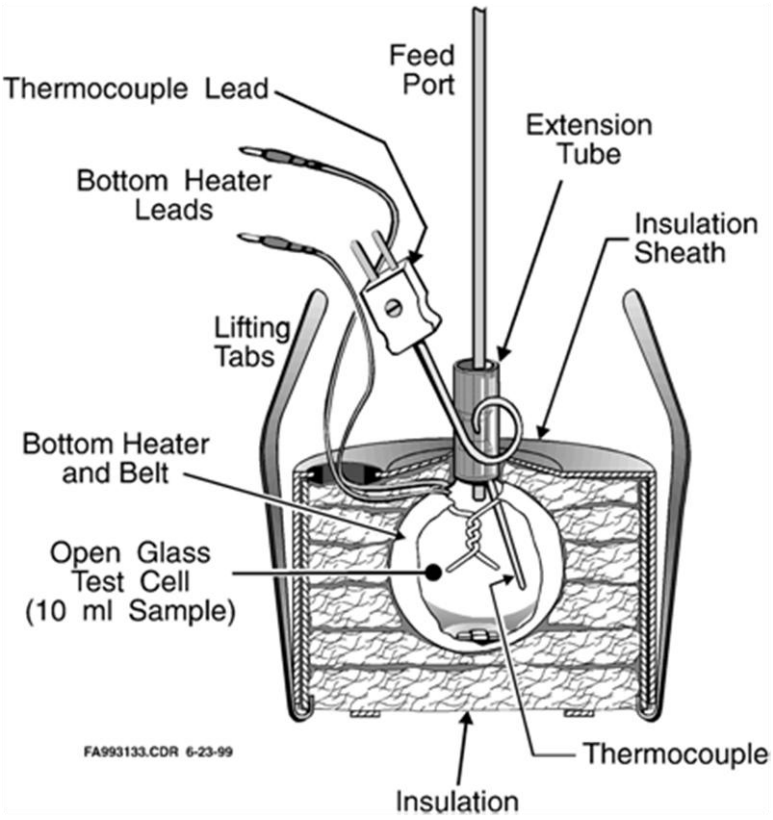

Figure 13 Test cell assembly [with permission from Fauske & Associates, Inc.]

After the sample is loaded, the containment vessel is pressurized with nitrogen to 250-300 psig to mitigate the boil-off as well as sample loss from the test cell. Then, sample is heated up at a constant ramp rate. In order to shorten the total time of a test run, a mode of high ramp rate followed by low ramp rate can be applied. The heat ramp rate is switched from high level to low level to ensure the sensitivity of the equipment when the temperature of the sample is close the onset temperature. Experiment shutdown criteria can be customized to decide the time to turn off heater and quit the program.

Figure 14 RSST™ including pressure vessel and control unit

(Source: http://www.chem.mtu.edu/~crowl/rsst.htm)

3.4.2 Thermal inertia

Thermal inertia is a term used to describe the property related to thermal conductivity and volumetric capacity of bulk material. It is known that in calorimeter test, part of the heat loss is caused by heating up of test cell. Energy balance of the system is established to describe the heat loss in calorimeter test (Equation 10).

$$m_s C_s \Delta T_{ad,adj} = (m_s C_s + m_c C_c)\Delta T_{ad,meas} \quad \textbf{(10)}$$

m_s: sample mass

C_s: heat capacity of sample

C_c: heat capacity of test cell

$\Delta T_{ad,meas}$: adiabatic temperature rise measured of the overall system

$\Delta T_{ad,adj}$: adjusted adiabatic temperature rise

So, the thermal inertia factor, ϕ, can be defined as:

$$\phi = \frac{(m_s C_s) + (m_c C_c)}{(m_s C_s)} \quad \textbf{(11)}$$

Using thermal inertia, the adiabatic temperature rise measured and the adjusted adiabatic temperature rise can be converted to each other using Equation 12. The high value of ϕ is equal to 1 under ideal adiabatic condition. The inverse of thermal inertia, is defined as the degree of adiabaticity.

$$\Delta T_{ad,adj} = \phi \Delta T_{ad,meas} \quad \textbf{(12)}$$

Temperature of systems with different ϕ can be converted to each other using Equation 13.

$$T_2 = T_{O,2} + \left(\frac{\phi_1}{\phi_2}\right)\left(T_1 - T_{O,1}\right) \quad \textbf{(13)}$$

For the same self-heat rate in adiabatic environment, the performance of reactions in calorimetry tests with different values of ϕ are different (Equation 14). To compare onset temperatures determined by different calorimeters, Equation 15 was derived to realize this conversion based on Equation 14.

$$\left.\frac{dT}{dt}\right|_{\phi 1} = \left.\frac{dT}{dt}\right|_{\phi 2} \quad \textbf{(14)}$$

$$\Rightarrow A\exp\left(\frac{-E_a}{RT_{\phi 1}}\right)\left(\frac{T_{\max,\phi 1}-T_{\phi 1}}{\Delta T_{ad,\phi 1}}\right)\Delta T_{ad,\phi 1}C_0{}^{n-1} = A\exp\left(\frac{-E_a}{RT_{\phi 2}}\right)\left(\frac{T_{\max,\phi 2}-T_{\phi 2}}{\Delta T_{ad,\phi 2}}\right)\Delta T_{ad,\phi 2}C_0{}^{n-1}$$

$$\Rightarrow \frac{1}{T_{o,2}} = \frac{1}{T_{o,1}} + \frac{R}{E_a}\ln\left(\frac{\phi_1}{\phi_2}\right) \quad \textbf{(15)}$$

The self-heat rate can also be converted between tests with different ϕ values using Equation 16. This is usually applied to the conversion of maximum self-heat rate in calorimetry tests.

$$\left.\frac{dT}{dt}\right|_{\phi 2} = \left(\frac{\phi_1}{\phi_2}\right)\exp\left[\frac{E}{R}\left(\frac{1}{T_{\phi 1}}-\frac{1}{T_{\phi 2}}\right)\right]\left.\frac{dT}{dt}\right|_{\phi 1} \quad \textbf{(16)}$$

Using the same principle, parameters like maximum temperature and heat generation of reactions can be corrected by taking thermal inertia into account.

$$T_{\max} = T_{o,adj} + \phi\Delta T_{ad,meas} \quad \textbf{(17)}$$

$$\Delta_r H = mC_c\phi\Delta T_{ad,meas} \quad \textbf{(18)}$$

The time to maximum reaction rate can be adjusted to ideal adiabatic environment using Equation 19.

$$TMR_{ad,adj} = \frac{TMR_{ad,meas}}{\phi} \quad \textbf{(19)}$$

CHAPTER IV

COMPUTATIONAL RESEARCH ON DECOMPOSITION REACTION MECHANISM OF CUMENE HYDROPEROXIDE

4.1 Introduction

The reaction mechanism of CHP decomposition has been studied by different researchers. Using experimental analysis method, the decomposition reaction mechanism was studied in presence of different solvents and contaminants[6, 7, 17, 18, 36]. However, because of the instability of intermediates in the decomposition reaction, it was difficult to investigate the reaction mechanism in detail. With the help of computational quantum chemistry method, it is possible to study the intermediates involved in the decomposition reaction and the elementary reactions. Based on the information obtained through quantum chemistry method, the mechanism of the decomposition reaction can be studied, including the research on thermodynamic stability and kinetic stability.

4.2 Result and discussion

Based on the proposed CHP decomposition reaction mechanism (Figure 15), a picture of postulated reaction pathways can be drawn (Figure 16)[10]. In order to yield estimation of Gibbs free energy and enthalpy, different computational quantum chemistry methods were applied to each molecule involved in the reaction mechanism. The computed result of Gibbs free energy and enthalpy in ideal gas phase are listed in Table 2 and Table 3. Based on these data, Gibbs free energy change and enthalpy change of each possible

elementary reaction in a decomposition mechanism was calculated, as listed in Table 4 and Table 5.

i $C_6H_5C(CH_3)_2OOH \rightarrow C_6H_5C(CH_3)_2O\bullet + \bullet OH$

ii $C_6H_5C(CH_3)_2O\bullet \rightarrow C_6H_5COCH_3 + \bullet CH_3$

iii $C_6H_5C(CH_3)_2H + \bullet CH_3 \rightarrow CH_4 + C_6H_5C(CH_3)_2\bullet$

iv $C_6H_5C(CH_3)_2H + \bullet OH \rightarrow H_2O + C_6H_5C(CH_3)_2\bullet$

v $C_6H_5C(CH_3)_2O\bullet + C_6H_5C(CH_3)_2H \rightarrow C_6H_5C(CH_3)_2OH + C_6H_5C(CH_3)_2\bullet$

vi $C_6H_5C(CH_3)_2O\bullet + \bullet OH \rightarrow C_6H_5OH + CH_3COCH_3$

vii $C_6H_5C(CH_3)_2\bullet + \bullet OH \rightarrow C_6H_5CH_3C=CH_2 + H_2O$

viii $2C_6H_5C(CH_3)_2\bullet \rightarrow [C_6H_5C(CH_3)_2]_2$

Figure 15 Elementary reactions involved in CHP decomposition reaction

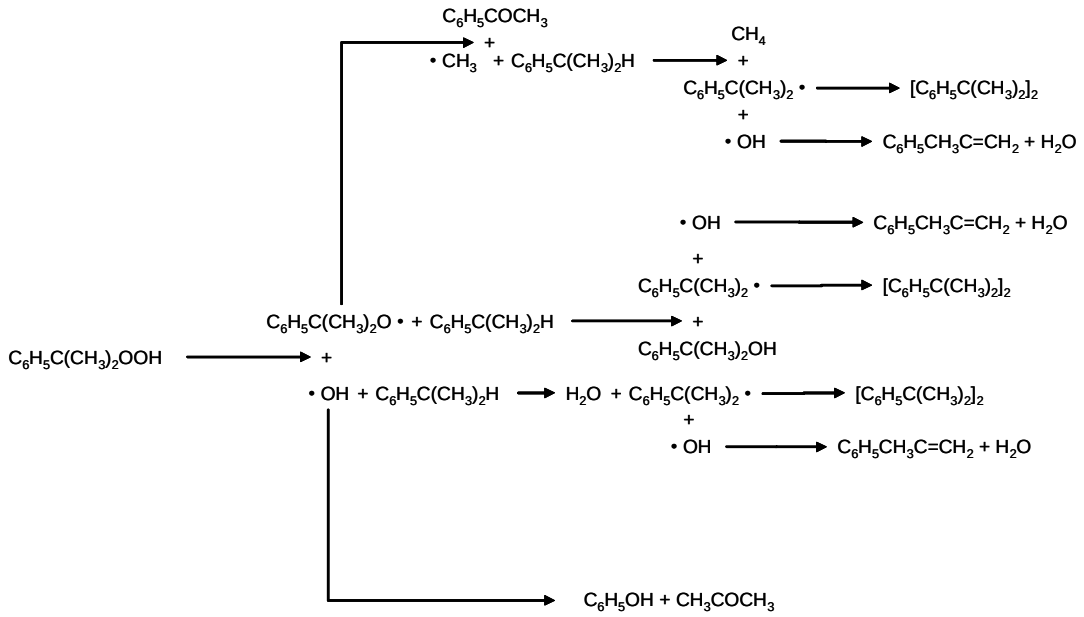

Figure 16 Posulated reaction pathways of CHP decomposition

Table 2 Gibbs free energy of CHP decomposition components calculated using four levels of theory

Component	Gibbs free energy of component (Hartree)*			
	AM1	HF/6-31G(d)	B3LYP/6-31G(d)	CBS-4M
$C_6H_5C(CH_3)_2OOH$	0.146900	-497.250000	-500.380000	-499.810000
$C_6H_5(CH_3)_2O\cdot$	NA	-421.891000	-424.599000	-424.082000
$\cdot OH$	-0.007630	-75.390100	-75.732100	-75.675400
$C_6H_5COCH_3$	0.083079	-382.361000	-384.790000	-384.321000
$\cdot CH_3$	0.059781	-39.546300	-39.826600	-39.778700
$C_6H_5C(CH_3)_2H$	0.160845	-347.643000	-350.041000	-349.603000
CH_4	0.012999	-40.164700	-40.490500	-40.446500
$C_6H_5C(CH_3)_2\cdot$	0.171478	-347.064000	-349.413000	-348.945000
H_2O	-0.091630	-76.005400	-76.405500	-76.367600
$C_6H_5C(CH_3)_2OH$	0.100328	-422.491000	-425.249000	-424.756000
C_6H_5OH	0.042214	-305.475000	-307.389000	-307.028000
CH3COCH3	-0.021230	-191.901000	-193.100000	-192.890000
$C_6H_5CH_3CCH_2$	0.182487	-346.481000	-348.835000	-348.389000
$[C_6H_5C(CH_3)_2]_2$	0.368768	-694.092000	-698.851000	-697.996000

* Hartree = 627.51 kcal/mol

The reference state used for all calculation conducted in this thesis: 298.15 K, 1 atmosphere, ideal gas phase.

Table 3 Enthalpy of CHP decomposition components calculated using four levels of theory

Component	enthalpy of component (Hartree) *			
	AM1	HF/6-31G(d)	B3LYP/6-31G(d)	CBS-4M
$C_6H_5C(CH_3)_2OOH$	0.195780	-497.200000	-500.330000	-499.760000
$C_6H_5(CH_3)_2O\cdot$	NA	-421.847000	-424.555000	-424.036000
$\cdot OH$	0.012545	-75.369900	-75.711800	-75.655200
$C_6H_5COCH_3$	0.125601	-382.320000	-384.749000	-384.280000
$\cdot CH_3$	0.081716	-39.523800	-39.804400	-39.756500
$C_6H_5C(CH_3)_2H$	0.204424	-347.601000	-349.998000	-349.560000
CH_4	0.034185	-40.1436000	-40.469400	-40.425400
$C_6H_5C(CH_3)_2\cdot$	0.216170	-347.019000	-349.368000	-348.900000
H_2O	-0.070210	-75.984000	-76.384000	-76.346200
$C_6H_5C(CH_3)_2OH$	0.146196	-422.447000	-425.204000	-424.711000
C_6H_5OH	0.077822	-305.440000	-307.354000	-306.992000
CH3COCH3	0.011485	-191.866000	-193.065000	-192.856000
$C_6H_5CH_3CCH_2$	0.224911	-346.440000	-348.793000	-348.347000
$[C_6H_5C(CH_3)_2]_2$	0.430630	-694.033000	-698.790000	-697.935000

* Hartree = 627.51 kcal/mol

4.2.1 Thermodynamic stability

From the data of Gibbs free energy in Table 4, it can be concluded that all the elementary reactions are thermodynamically feasible except reaction i (Figure 15), because of negative Gibbs free energy change. For reaction viii, the Gibbs free energy change calculated is positive using AM1 and HF method. However, reaction viii is still determined to be thermodynamically feasible because of negative Gibbs free energy obtained using other two more advanced theory levels. In ideal gas phase, elementary

reaction i, the initiation step of decomposition reaction, is thermodynamically infeasible because of positive Gibbs free energy change. However, as Gibbs free energy varies linearly with temperature, it will become negative if temperature rises up to an appropriate level. This agrees with the phenomenon that CHP is stable under atmospheric temperature but begins to decompose in the environment of high temperature. The thermodynamic feasibility of reaction i was also validated by previous research[17, 37]. Therefore, based on the analysis of data obtained through four different levels of computational quantum chemistry method, it can be concluded that every elementary reaction in postulated mechanism is thermodynamically feasible in practical environment.

Table 4 Gibbs free energy change of elementary reactions of CHP decomposition calculated using four levels of theory

reaction	Gibbs free energy change of elementary reaction (kcal/mol)			
	AM1	HF/6-31G(d)	B3LYP/6-31G(d)	CBS-4M
i	NA	-22.8	28.0	34.0
ii	NA	-9.6	-10.9	-11.3
iii	-22.7	-24.7	-22.2	-6.2
iv	-46.0	-22.7	-28.2	-21.5
v	NA	-12.9	-13.1	-10.4
vi	NA	-58.8	-99.0	-100.7
vii	-45.8	-20.2	-59.9	-85.1
viii	16.2	22.9	-15.8	-65.8

Enthalpy change of each elementary reaction can be calculated based on data in Table 3. By analysis of the enthalpy change data (Table 5), reaction i was found to be endothermic. Reaction ii cannot be determined to be exothermic or endothermic because the enthalpy change calculated using B3LYP/6-31G(d) and CBS-4M method does not agree with each other. Considering the small value of enthalpy change of reaction ii, its exothermic or endothermic behavior should be very weak. It needs to be noticed that there are three extraordinary exothermic elementary reactions, reaction vi, vii and viii. These three reactions have to be scrutinized in the research of kinetic stability since it is possible that these extreme exothermic reactions cannot be addressed by Polanyi equation or Marcus equation.

Table 5 Enthalpy change of elementary reactions of CHP decomposition calculated using four levels of theory

Component	enthalpy change of elementary reaction (kcal/mol)			
	AM1	HF/6-31G(d)	B3LYP/6-31G(d)	CBS-4M
i	NA	-11.6	38.2	44.4
ii	NA	2.00	1	-0.1
iii	-22.4	-23.9	-21.8	-5.6
iv	-44.6	-20.4	-26.3	-19.4
v	NA	-11.7	-11.7	-9.2
vi	NA	-55.9	-95.5	-98.2
vii	-46.4	-21.6	-61.2	-86.2
viii	-1.1	3.8	-34.0	-84.3

4.2.2 Kinetic stability

In order to carry out complete hazards evaluation on reaction mechanism, besides thermodynamic stability, kinetic stability has to be analyzed as well. As an important parameter presenting the kinetic stability of reaction, activation energy of each elementary reaction was calculated using both Polanyi equation and Marcus equation. Intrinsic activation energy (E_a^0) and transfer coefficient (γ_p) were chosen from literature according to the types of reactions[38]. In most cases, compared with AM1 and HF methods, DFT and CBS methods are more accurate and reliable for prediction of energy and other thermodynamic parameters of molecules. Therefore, enthalpy change calculated using B3LYP/6-31G(d) and CBS-4M method were applied to the activation energy evaluation. The result is shown in Table 6 and Table 7.

It should be noted that the application of Polanyi equation and Marcus equation to evaluation of activation energy of reactions yielded some unrealistic values for reaction vii and viii. This might be caused by the extraordinary exothermicity of these reactions which cannot be addressed by Polanyi equation or Marcus equation.

The first step of the reaction mechanism is believed to be the rate-determining step of the whole reaction by former researchers[11, 17]. After the initiation step, radical $C_6H_5C(CH_3)_2O\cdot$ produced by the first step faces three thermodynamically feasible routes: it can decompose further via reaction ii; it can react with cumene to create new radical via reaction v; or it can join the termination reaction vi to form final products.

Comparing activation energy of these three elementary reactions, it is found that the activation energy for reaction ii is much lower than that of reaction v and vi. So, under the same reaction condition, the reaction ii is much more competitive and consumes most of the radical $C_6H_5C(CH_3)_2O\cdot$ produced.

For the radical ·OH produced by the initial step, there are three possible reaction routes, one is to react with cumene via reaction iv; one is to react with $C_6H_5C(CH_3)_2O\cdot$ to form acetone and phenol via reaction vi; another one is to follow termination reaction vii. According to activation energy data, reaction vi and vii have much higher energy barrier than that of reaction iv. So, it can be concluded that the proportion of radical ·OH that reacts with cumene via reaction iv is much larger than that follows the reaction vi and vii.

Two termination reactions, reaction vii and viii, share the same reactant $C_6H_5C(CH_3)_2\cdot$, By comparison of these two activation energies, it is revealed that reaction viii is more competitive than reaction vii, but not overwhelming. But considering the fact that reaction vii is already depressed by reaction iv, it is a reasonable conclusion that reaction viii is the overwhelming one between these two reactions.

Table 6 Activation energy of CHP decomposition elementary reactions calculated using the Polanyi and Marcus equations and the B3YLP/6-31G(d) enthalpy of reaction

Component	Transfer coefficient, γ_p	Intrinsic activation energy, E_a^0	Activation energy of reaction, E_a (kcal/mol)	
			Polanyi Equation	Marcus Equation
i	1	1	39.2	111.4
ii	1	1	2.0	1.6
iii	0.3	12	5.4	3.6
iv	0.3	12	4.1	2.4
v	0.3	12	8.5	6.9
vi	0.5	50	2.2	13.6
vii	1	2	-	88.3
viii	0	1	1	56.2

-: unrealistic value

Table 7 Activation energy of CHP decomposition elementary reactions calculated using the Polanyi and Marcus equations and the CBS-4M enthalpy of reaction

Component	Transfer coefficient, γ_p	Intrinsic activation energy, E_a^0	Activation energy of reaction, E_a (kcal/mol)	
			Polanyi Equation	Marcus Equation
i	1	1	45.4	146.3
ii	1	1	0.9	0.9
iii	0.3	12	10.3	9.4
iv	0.3	12	6.2	4.2
v	0.3	12	9.2	7.8
vi	0.5	50	0.9	12.9
vii	1	2	-	-
viii	0	1	1	-

Based on the kinetic analysis above, five elementary reactions, i, ii, iii, vi and viii are determined to be kinetic plausible elementary reactions in the CHP decomposition reaction mechanism. The formation of 2-Phenyl-2-propanol, acetone, phenol, alpha-methylstyrene are limited. The simplified decomposition reaction mechanism is shown is Figure 17.

$$C_6H_5C(CH_3)_2OOH \rightarrow C_6H_5C(CH_3)_2O\bullet + \bullet OH$$
$$C_6H_5C(CH_3)_2O\bullet \rightarrow C_6H_5COCH_3 + \bullet CH_3$$
$$C_6H_5C(CH_3)_2H + \bullet CH_3 \rightarrow CH_4 + C_6H_5C(CH_3)_2\bullet$$
$$C_6H_5C(CH_3)_2H + \bullet OH \rightarrow H_2O + C_6H_5C(CH_3)_2\bullet$$
$$2C_6H_5C(CH_3)_2\bullet \rightarrow \left[C_6H_5C(CH_3)_2\right]_2$$

Figure 17 Proposed reaction mechanism of CHP decomposition

The dominant reaction pathway consisting of these four kinetic plausible elementary reactions is as follows:

$$C_6H_5C(CH_3)_2OOH + 2C_6H_5C(CH_3)_2H \rightarrow C_6H_5COCH_3 + CH_4 + H_2O + \left[C_6H_5C(CH_3)_2\right]_2$$

Using enthalpy change of these four dominant elementary reactions calculated in three theory levels, enthalpy change of this dominant reaction pathway can be obtained. The results are listed in Table 8. According to this reaction, the mole of methane produced in the runaway reaction is equal to the mole of CHP consumed. Final products derived

from dominant reaction pathway agree with experimental result of previous research that methane and acetophenone are major components of CHP decomposition products[10].

Table 8 Enthalpy change of dominant reaction pathway calculated in four levels of theory for CHP decomposition

Level of theory	Enthalpy of reaction pathway (kcal/mol)
HF/61-31G(d)	-50.1
B3LYP/61-31G(d)	-43.0
CBS-4M	-65.1

As results obtained in Table 8 are purely based on computational quantum chemistry method, experimental data need to be applied to the validation of the dominant reaction pathway. It was reported that the experimental value of enthalpy change of CHP decomposition is about 68.1 kcal/mol[10]. The prediction result was compared with this data. The result of the comparison is shown in Table 9.

Table 9 Comparison of prediction value with empirical data for CHP decomposition reaction enthalpy change in two four levels of theory

Level of theory	Prediction value/ empirical data (%)
HF/61-31G(d)	73.6
B3LYP/61-31G(d)	63.0
CBS-4M	95.5

The data from Table 9 shows that the ratio between predicted value and empirical data varies from 63% to 95.5 %. This result indicates that prediction of enthalpy change derived from dominant reaction pathway is quite close to empirical data. However, it should be noticed that the predicted enthalpy change was calculated in ideal gas phase, which does not include the heat of vaporization. By taking the heat of vaporization into account, the final predicted enthalpy change should be lower than present value. Though heat of vaporization is supposed to be much smaller than enthalpy change calculated in ideal gas phase, quantitative validation is still needed to support this assumption. In order to validate the postulated dominant reaction pathway, the predicted enthalpy needs to be corrected by the term of heat of vaporization and compared with experimental data. Also, because the enthalpy changes are different in the levels of B3LYP/61-31G(d) and CBS-4M, calculation in more advanced level such as G2 is expected to be carried out to ensure the accuracy of the theoretical calculation.

4.3 Conclusion

Using computational quantum chemistry as an effective tool, fundamental research can be conducted on the reaction mechanism of CHP decomposition, which was difficult to be investigated earlier because of unstable radicals in the reaction mechanism.

According to the analysis of thermodynamic and kinetic stability of CHP decomposition reaction mechanism, a dominant reaction pathway was determined, which is not only thermodynamically feasible but also kinetically plausible. This dominant reaction pathway agrees with the experimental result that methane and acetophenone are major components of CHP decomposition products. Also, the prediction of enthalpy change of this reaction pathway is close to experimental data in all four theory levels.

Some valuable information can be derived from the dominant reaction pathway. According to the stoichiometry of the reaction pathway, the ratio between CHP and cumene is 1 to 2. This indicates CHP decomposition reaction only follows this reaction pathway when there is sufficient cumene. If the ratio between CHP and cumene is less than 1 to 2, unknown decomposition reactions pathway might be involved in CHP decomposition reaction.

Another important prediction based on postulated reaction pathway is the gas generation. According to the reaction equation, the mole of methane generated in reaction process is equal to the mole of the CHP consumed if there is sufficient cumene. This conclusion is

the theoretical basis for the prediction of non-condensable pressure. The non-condensable pressure is the difference between the pressure before the runaway reaction and the pressure after the completion of reaction under a certain temperature. The non-condensable pressure is an estimation of the gas generation, which rules out the influence of reaction heat. It is also a good way to validate the postulated reaction pathway using the parameter of non-condensable pressure, which will be included in the future work.

CHAPTER V

EVALUATION OF CHP REACTIVITY HAZARDS

5.1 Introduction

CHP is a hazardous material for industrial process because of its sensitivity to heat and incompatibility to contaminants. Any improper management or operation might trigger runaway reactions in the process of production, transportation or storage. Therefore, it is of great importance to evaluate the reactivity hazards of CHP decomposition reaction. The evaluation results can be used to prevent the occurrence of runaway reaction. Also, it is necessary to introduce the evaluation results into design of related equipment as well as development of industrial codes.

In this research, calorimetry tests using RSST^{TM} were carried out to evaluate the reactivity hazards of CHP. Considering the importance of operation parameters in process safety, the effect of CHP concentration was chosen as the focal point for hazards evaluation. The effect of CHP concentration on onset temperature, an important parameter to prevent runaway reaction, was studied in this research. Also the effect of CHP concentration on exothermic behavior of runaway reactions was investigated. The objective is to get a comprehensive understanding of the effect of CHP concentration, which can be applied to industrial process.

In this research, concentration range of CHP was chosen as 12-80 wt%. 80 wt% is the highest concentration encountered in CHP production. The lower concentration of 12

wt% was selected so that the results from this research can be compared against previous research (12-35%)[9].

5.2 Sample

Aldrich 88 % CHP, catalog number 513296, was employed in the experimental research. Fisher 99.9 % cumene, catalog number AC-32973-5000, was used as dilution solvent in the experiment.

The summary of experimental data for sample and thermal inertia ϕ is presented in Table 10.

Table 10 Summary of sample weight and thermal inertia

Concentration (wt%)	Test No.	Weight of test cell (g)	Sample weight (g)	ϕ
12	1	1.54	4.6	1.13
	2	1.55	4.62	1.13
	3	1.52	4.61	1.12
20	1	1.47	4.63	1.12
	2	1.43	4.61	1.12
	3	1.39	4.6	1.11
30	1	1.51	4.62	1.12
	2	1.38	4.62	1.11
	3	1.49	4.59	1.12

Table 10 continued

Concentration (wt%)	Test No.	Weight of test cell (g)	Sample weight (g)	ϕ
40	1	1.50	4.61	1.12
	2	1.44	4.59	1.12
	3	1.50	4.59	1.12
50	1	1.48	4.61	1.12
	2	1.44	4.63	1.12
	3	1.32	4.61	1.11
60	1	1.49	4.62	1.12
	2	1.48	4.64	1.12
	3	1.46	4.63	1.12
70	1	1.42	4.59	1.12
	2	1.43	4.60	1.12
	3	1.44	4.59	1.12
80	1	1.39	4.63	1.11
	2	1.34	4.60	1.11
	3	1.47	4.60	1.12

5.3 Operation mode

i. Before test, pressure containment should be pressurized by nitrogen up to 300 psi.

ii. The ramp rate is set at 2 °C/min in the temperature interval of 0 to 90 °C. In the temperature interval higher than 90 °C, the ramp rate is 0.5 °C /min.

iii. The heater will be turned off automatically if one of the following conditions is satisfied.

1. Running time is longer than 250 min.
2. Temperature of the test is higher than 480 °C.
3. Pressure of the test is higher than 500 psi.

iv. The system will automatically save data and quit the program once the temperature is lower than 25 °C after the heater is turned off.

5.4 Experimental results and analysis

Experiments were performed in RSST^{TM} to determine the effect of CHP concentration on runaway reactions. Eight different initial concentrations were included in this research: 12, 20, 30, 40, 50, 60, 70, 80 wt%.

5.4.1 Temperature analysis

Figure 18 shows the temperature profiles of RSST^{TM} tests in different concentrations. By comparison of these profiles, a phenomenon observed is that the exothermic behavior of the runaway reaction becomes stronger with the increase of CHP concentration. This tendency is quite clear in the range of low concentration. In the test of 12 wt% CHP, the temperature profile is pretty smooth and moderate. However, this curve becomes much sharper in the test of 20 wt% CHP and reached much higher temperature peak value. The tendency remains the same until the concentration is raised to 40 wt%. Above the concentration of 40 wt%, there is no significant difference between the temperature profiles of the tests. This phenomenon agrees with the numerical analysis result of maximum temperature of the runaway reactions (Table 11). By plotting the maximum

temperature versus CHP concentration, two divisions can be identified (Figure 19). In the concentration range below 40 wt%, a considerable increase from 200 to 300 °C of maximum temperature can be observed. Whereas over the concentration range of 40 to 80 wt%, the maximum temperature has only insignificant change from 299 °C to 337 °C. The change of the temperature profile over concentration is reasonable according to theoretical postulation. As the total weight of the sample is similar in each test, more CHP is involved in decomposition reaction with the increase of CHP concentration. Considering CHP decomposition reaction is a self-accelerating reaction, the reaction rate keeps increasing until the depletion of the reactants. With more reactant involved in decomposition reaction, the release of heat becomes faster and fiercer, and higher maximum temperature can be reached at the end of the reaction. However, the change of exothermic behavior across 40 wt% is an interesting phenomenon which cannot be explained by the kinetic knowledge mentioned above. This phenomenon was observed in almost all important parameters and is discussed in the conclusion part of this chapter.

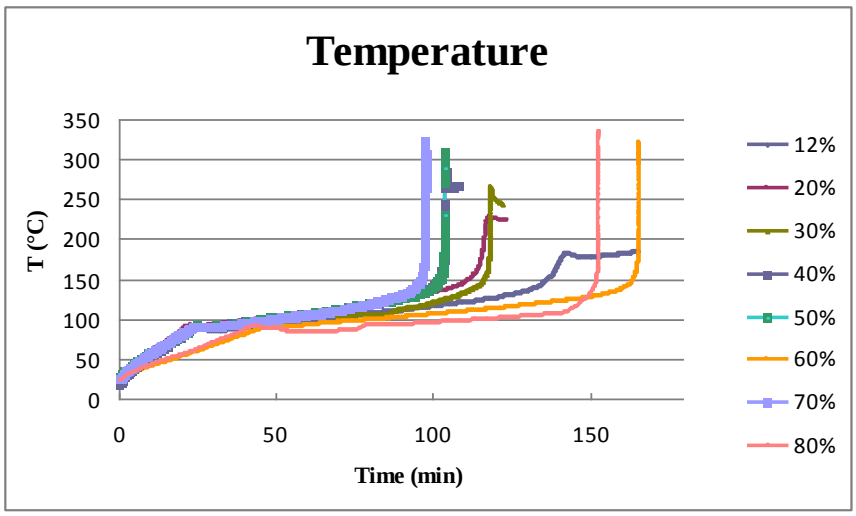

Figure 18 Temperature profile of RSST™ tests at different CHP concentrations

Table 11 Maximum temperature for different CHP concentrations

Concentration (wt %)	T_{max} (°C)	δ (°C)
12	199.5	11.7
20	234.5	5.8
30	262.6	7.7
40	299.0	2.0
50	311.1	3.5
60	316.5	5.3
70	321.9	1.7
80	337.0	6.0

δ: standard deviation

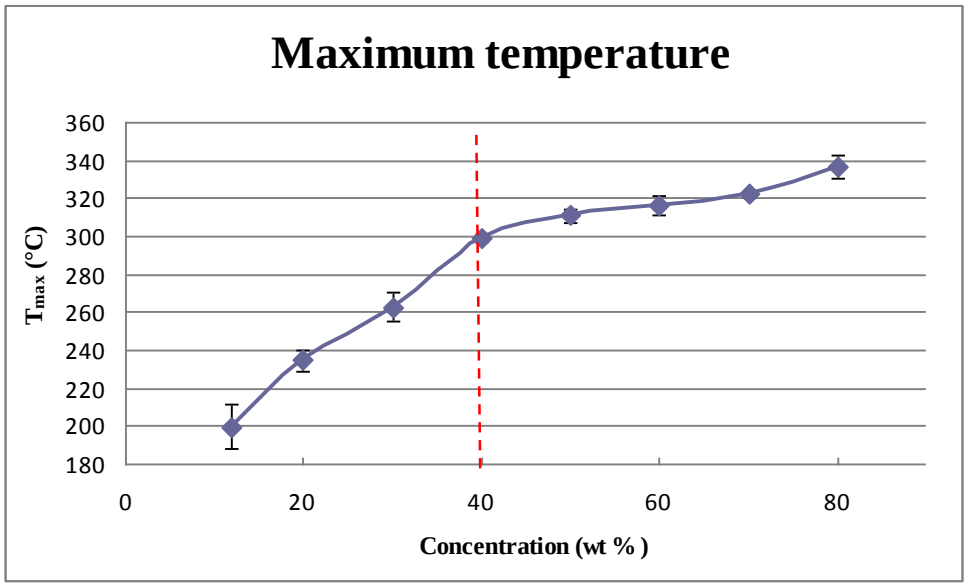

Figure 19 Effect of CHP concentration on the maximum temperature

Onset temperature, a critical parameter used to prevent runaway reactions, was determined by the temperature profiles (Table 12, Figure 20). Numerically, onset temperature does not vary greatly over concentration range according to the experimental results. Considering the small difference between onset temperature and operation temperature in industry process, it is still of great importance to study the change of the onset temperature over concentration range, which could be applied to industry process as a guideline for precise control of process temperature.

Table 12 Onset temperature for different CHP concentrations

Concentration (wt %)	T_{on} (°C)	δ (°C)
12	133.8	2.1
20	133.5	0.7
30	130.1	1.7
40	129.0	0.9
50	121.4	1.7
60	118.0	3.7
70	117.5	0.3
80	108.3	4.0

δ: standard deviation

Onset temperature remains above 129 °C with little change in the concentration range from 12 to 40 wt%. Once CHP concentration exceeds 40 wt%, a slow but observable decrease was detected in RSST^{TM} tests. Finally, the onset temperature can reach as low as 108.3 °C in 80 wt% CHP solution. This tendency is particularly important for condensation unit of CHP, where CHP solution (35 wt%) is concentrated up to 80 wt%. Therefore, in condensation process or other processes where considerable variance of concentration exists in the range of 40 to 80 wt%, it is important to keep the process operating temperature lower than the onset temperature of the highest concentration in the process. In order to get more accurate assessment for onset temperature of CHP solution in different concentrations, further research using more advanced equipment such as APTAC or ARC is recommended.

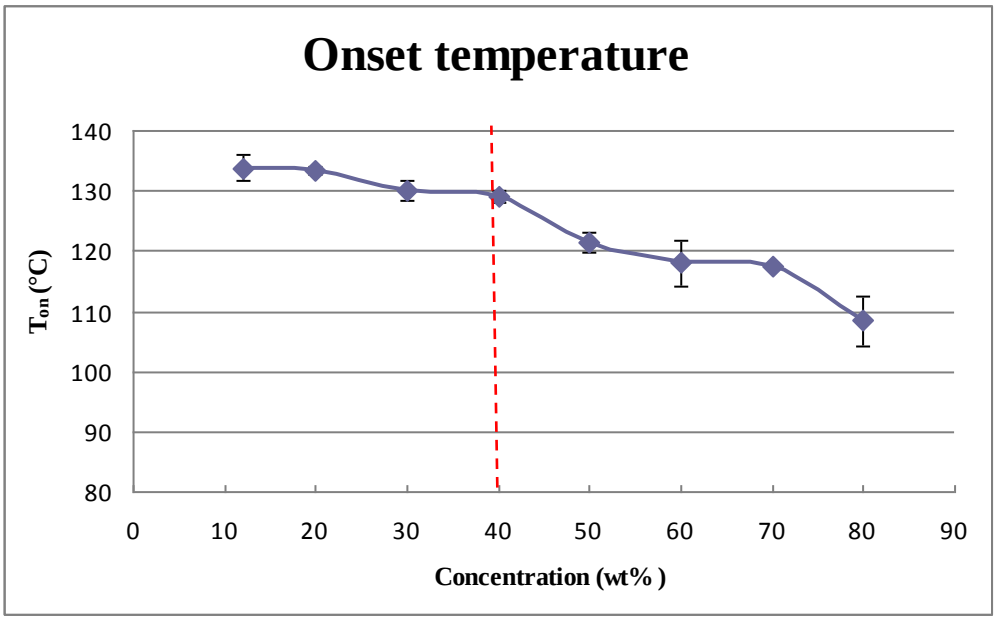

Figure 20 Effect of CHP concentration on the onset temperature

The maximum temperature increase is the difference between onset temperature and maximum temperature reached in the runaway reaction process in the same test. Because onset temperature does not change greatly over the concentration range (108.3-133.8 °C), the similar phenomenon was observed with maximum temperature increase that 40 wt% is a critical point (Table 13, Figure 21). The maximum temperature increases almost linearly with the increase of concentration in the range of 12 to 40 wt%. When the concentration is higher than 40 wt%, this increase tendency becomes much slower.

Table 13 Maximum temperature increase for different CHP concentrations

Concentration (wt %)	ΔT_{max} (°C)	δ (°C)
12	65.7	11.8
20	98.8	3.6
30	132.5	8.0
40	179.0	2.1
50	189.8	4.0
60	198.5	3.0
70	204.4	1.6
80	228.7	9.9

δ: standard deviation

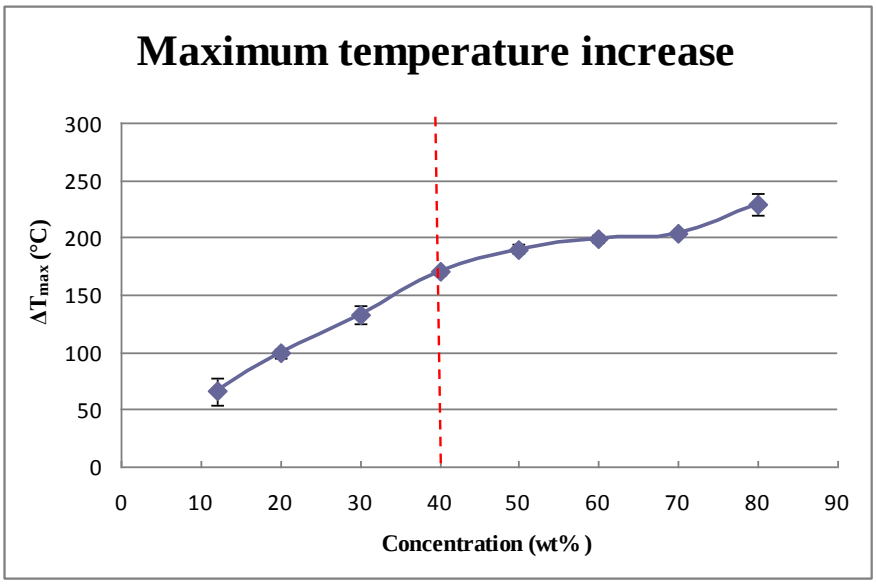

Figure 21 Effect of CHP concentration on the maximum temperature increase

5.4.2 Pressure analysis

Pressure profiles obtained by RSST^{TM} are shown in Figure 22. The pressure rise caused by runaway reaction was observed in all tests of different concentrations. In the concentration range from 12 to 40 wt%, the pressure of RSST^{TM} tests keeps at a relatively low level, with the maximum value varying from 314.9 to 357.7 psig. The increase of pressure is also moderate and smooth in this concentration range. Once the CHP concentration exceeds 40 wt%, there is a significant change in the shape of pressure curve. The pressure jumps up dramatically and even explosively once the runaway reaction is triggered. The maximum pressure of each RSST^{TM} test is summarized in Figure 23 and Table 14. Based on the analysis of numerical value and graph, 40 wt% of CHP concentration can still be regarded as a critical point for the effect of CHP concentration on pressure. The effect of CHP concentration on maximum pressure is obviously greater in the range lower than 40 wt% than in higher concentration range. The explanation for this is presented in conclusion part of this chapter.

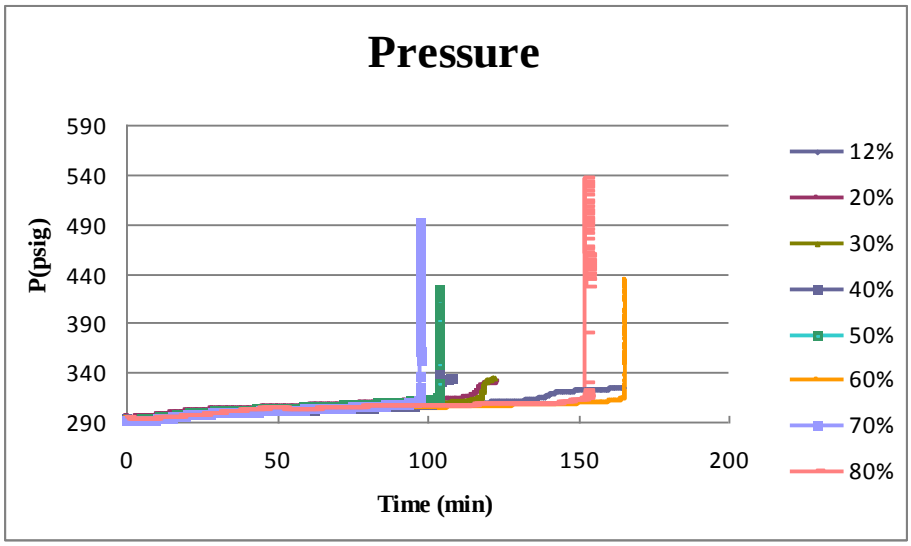

Figure 22 Pressure profiles of RSST™ tests at different CHP concentrations

Table 14 Maximum pressure for different CHP concentrations

Concentration (wt %)	P_{max} (Psig)	δ (Psig)
12	314.9	11.7
20	331.4	1.86
30	336.0	4.6
40	357.7	5.2
50	425.5	5.8
60	442.6	9.3
70	488.4	6.1
80	509.8	22.1

δ: standard deviation

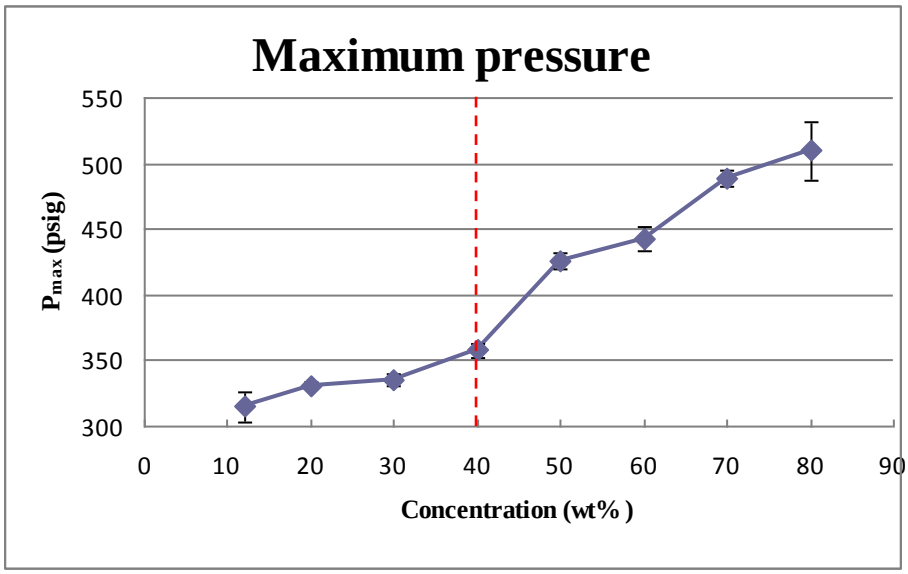

Figure 23 Effect of CHP concentration on the maximum pressure

The maximum pressure increase is the difference between the initial pressure of a runaway reaction and the maximum pressure reached in the runaway reaction process. The maximum pressure increase is a measurement of the pressure generation of runaway reactions. The curve of maximum pressure increase over concentration is similar with that of maximum pressure. Compared with lowest concentration of 12 wt%, maximum pressure increase reached almost 20 times when the concentration was raised to 80 wt%. The shape of the curve changes around 40 wt%, which can be viewed as a critical point. The experimental results are shown in Table 15 and Figure 24.

Table 15 Maximum pressure increase for different CHP concentrations

Concentration (wt %)	ΔP_{max} (Psig)	δ (Psig)
12	12.2	3.4
20	19.4	0.9
30	23.9	5.1
40	54.2	1.2
50	114.6	4.5
60	135.2	11.2
70	179.4	6.9
80	201.8	20.4

δ: standard deviation

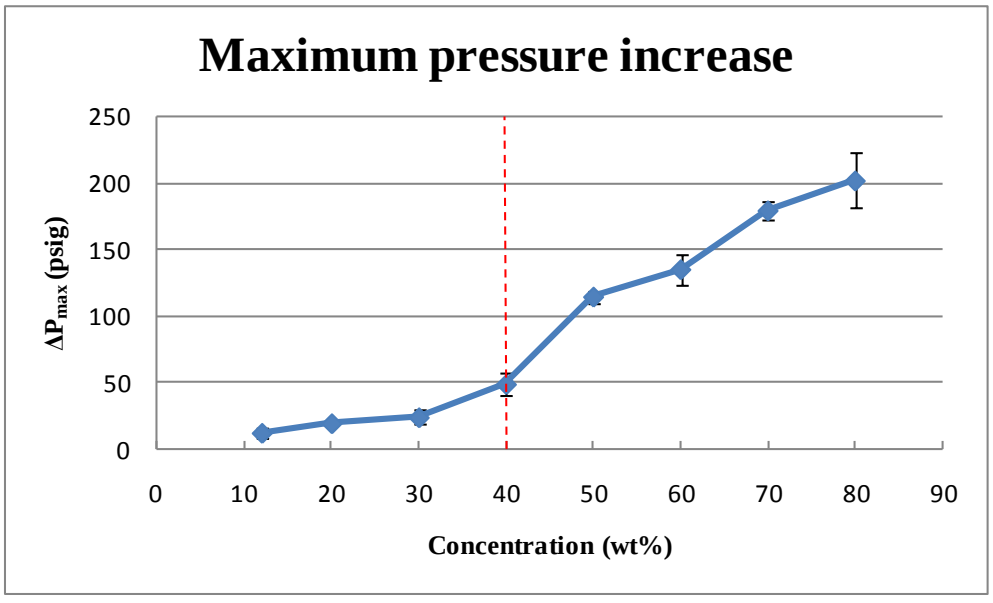

Figure 24 Effect of CHP concentration on the maximum pressure increase

5.4.3 Self-heat rate analysis

Self-heat rate profiles of RSST™ tests are shown and compared in Figure 25. The maximum self-heat rate is summarized in Table 16 and plotted in Figure 26 to clearly describe the self-heat rate of each test. With the increase of CHP concentration up to 40 %, a considerable increase of self-heat rate was observed in the process of runaway reactions. However, this tendency is not that clear and definite if the CHP concentration is above 40 wt%. This phenomenon agrees with temperature profiles mentioned previously.

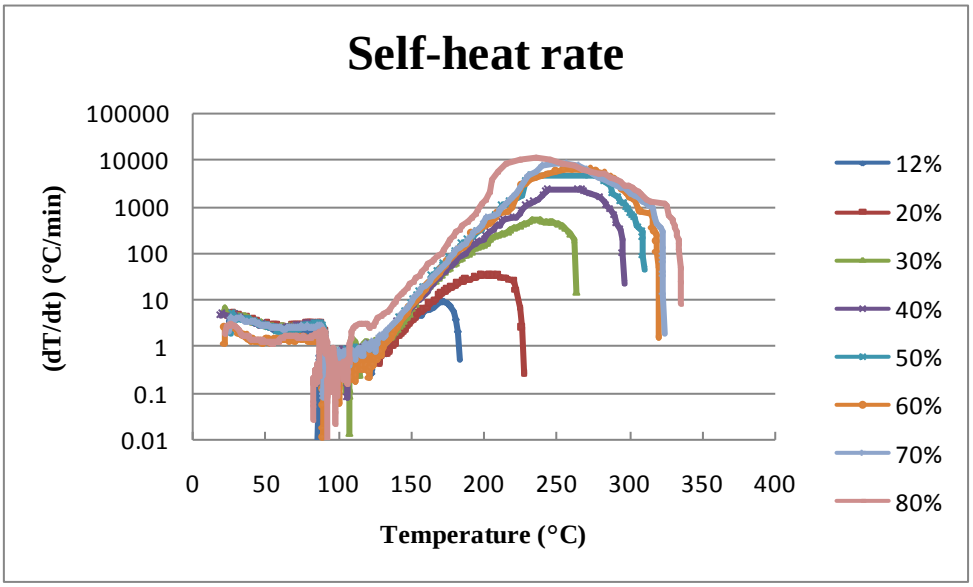

Figure 25 Self-heat rate profiles of RSST™ tests at different CHP concentrations

A plot in logarithmic scale of maximum self-heat rate can describe this phenomenon more clearly. In Figure 26, two different obvious tendencies can be observed. The

concentration effect on maximum self-heat rate follows an almost linear relationship over concentration when CHP concentration is below 40%. In this range, the maximum self-heat rate increases by 6 to 8 times between each two adjunct concentrations. Above 40 wt%, an observable but much slower increase of maximum self-heat rate was found over CHP concentration. Starting from 40 wt%, a total four-fold increase was observed when the concentration finally went up to 80 wt%.

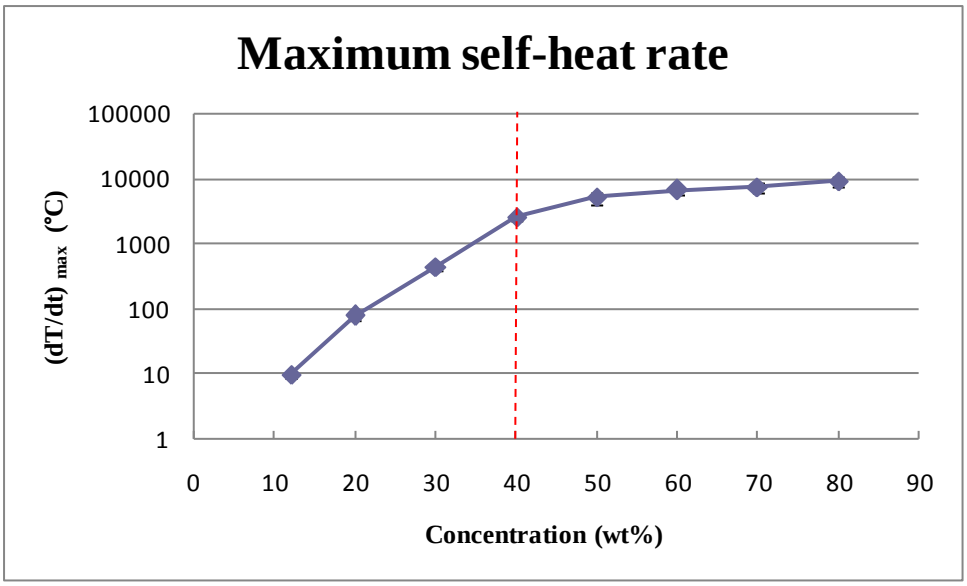

Figure 26 Effect of CHP concentration on the maximum self-heat rate

Table 16 Maximum self-heat rate for different CHP concentrations

Concentration (wt %)	$(dT/dt)_{max}$ (Psig/min)	δ (Psig/min)
12	9.7	1.1
20	77.6	12.0
30	445.3	50.5
40	2523.3	196.1
50	5128.3	1004.8
60	6694.7	950.7
70	7417.0	1453.9
80	9098.0	1603.2

δ: standard deviation

5.4.4 Pressure rate analysis

The pressure rate profiles are similar with that of self-heat rate (Figure 27). The point of 40 wt% can still be viewed as a critical point, beyond which the effect of CHP concentration on pressure rate changes. This conclusion is supported by the summarization presented in Figure 28 and Table 17, showing that the tendency of maximum pressure rate over concentration range changed around 40 wt%. The change of tendency is clearly presented by Figure 28 using logarithmic scale, where pressure rate remains in the same order of magnitude after rapid increase below 40 wt%.

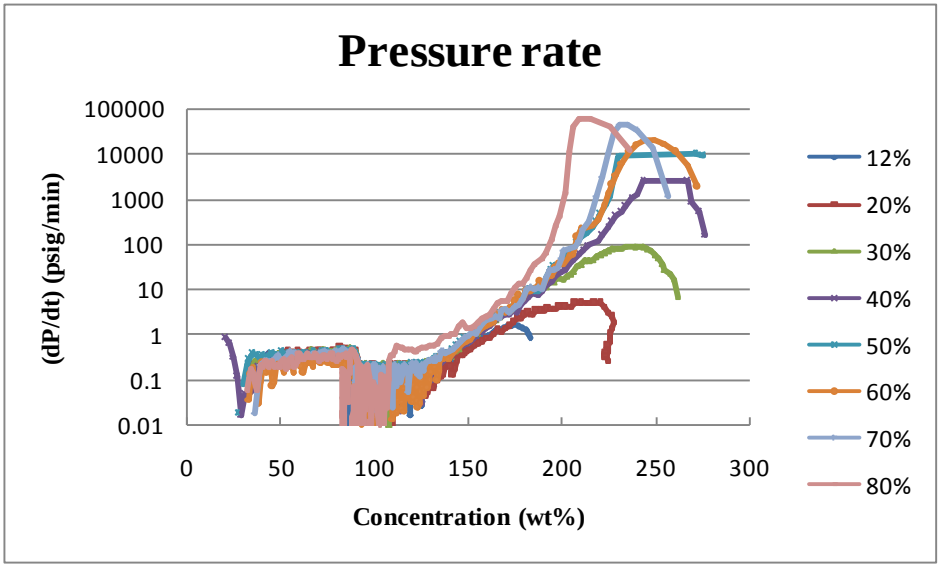

Figure 27 Pressure rate profiles of RSST™ tests at different CHP concentrations

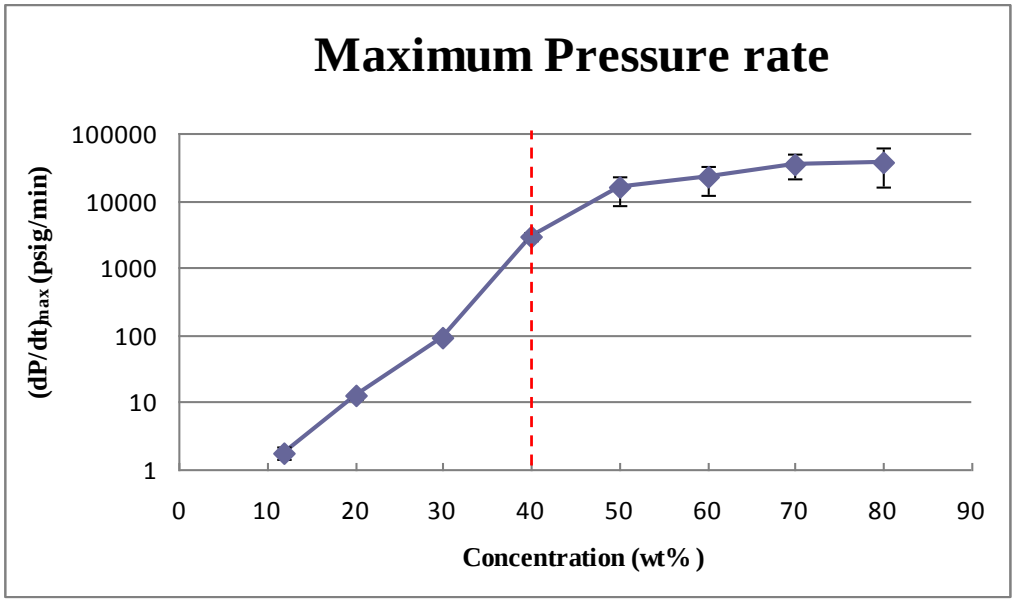

Figure 28 Effect of CHP concentration on the maximum pressure rate

Table 17 Maximum pressure rate for different CHP concentrations

Concentration (wt %)	$(dP/dt)_{max}$ (Psig/min)	δ (Psig/min)
12	1.8	0.3
20	12.4	0.9
30	92.3	6.1
40	2975.0	356.8
50	15838.3	7367.1
60	22333.3	10005.8
70	35800.0	14924.5
80	37875.0	22116.6

δ: standard deviation

5.5 Discussion and conclusion

Concentration, an important operation parameter for CHP solution in industrial process, varies greatly in different units or processes. According to previous research, it is believed that this parameter is able to influence the exothermic behavior of runaway reaction, and might also be an important factor for the onset temperature of CHP solution.

By carrying out a series of tests in RSST^{TM} over the wide CHP concentration range of 12 to 80 wt%, several important parameters such as onset temperature, maximum temperature, maximum pressure, maximum self-heat rate and maximum pressure rate, were obtained from the analysis of the RSST^{TM} tests results. Through analysis of experimental data, it was found that concentration of 40 wt% can be viewed as a critical

point for CHP concentration, because the exothermic behavior of runaway reaction over concentration changed around this point. Below the concentration of 40 wt%, the extent of exothermic behavior of runaway reaction is proportional to the concentration. However, this tendency is not that clear or becomes weaker once CHP concentration exceeds 40 wt%. This conclusion is supported by parameters of maximum temperature, maximum temperature increase self-heat rate and pressure rate. These parameters show a dramatic surge followed by a slow and smooth increase with increased CHP concentration. The parameters of maximum pressure and maximum pressure increase also follow the conclusion that 40 wt% is a critical point, but with different tendencies across that critical point. On the contrary, the increases of these two parameters are more dramatic in high concentration range (>40 wt%) than those in low concentration range (<40 wt%).

As the concentration of 40 wt% is a critical point for almost all important parameters of runaway reactions, the reaction mechanism might be a theoretical basis for the explanation of this phenomenon. By converting weight fraction into mole fraction, it is found that for 40 wt% CHP solution, the mole ratio between cumene and CHP is 1.9: 1, which is quite close to the ratio of 2: 1 predicted by reaction pathway proposed earlier. Therefore, it is speculated that the shift of reaction mechanism might be the major course for the change of exothermic behavior beyond 40 wt%. When CHP concentration is lower than 40 wt%, the reaction follows proposed reaction pathway. Once the concentration exceeds this critical point, part of the CHP follows some unknown

reaction pathways because of lack of cumene. With the increase of concentration in the range of 40 to 80 wt%, the percentage of CHP follows the unknown reaction pathway also increases (Figure 29). It is postulated that the alternative unknown reaction pathways might not be as exothermic as proposed dominant reaction pathway, which can be an explanation for slow increase of maximum temperature, maximum temperature increase, maximum self-heat rate and maximum pressure rate, when CHP concentration is above 40 wt%. Another speculation on alternative reaction pathway is that more gas generation might be involved in these unknown reaction pathways. This is helpful to figure out the different tendency that maximum pressure and maximum pressure increase surge more dramatically above 40 wt% of concentration.

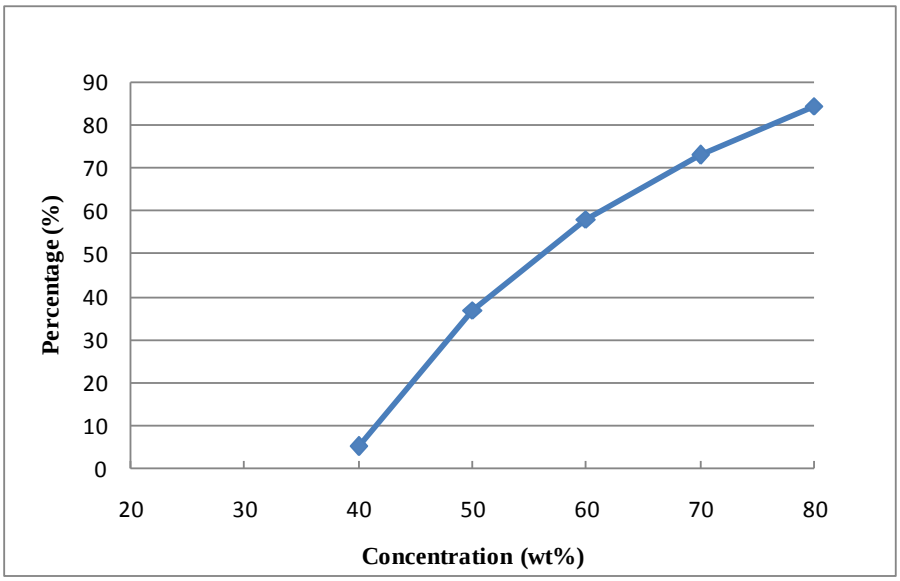

Figure 29 Percentage of CHP follow unknown reaction pathway

For onset temperature, the critical point of 40 wt% should not be caused by the unknown reaction pathways, as cumene is sufficient before the occurrence of runaway reaction. The onset temperature of CHP has only slight change below 40 wt%, but decreases obviously above 40 wt%. This is important for CHP condensation process, where CHP concentration varied within high concentration range (35-80 wt%). It will be effective to prevent runaway reaction by integrating this tendency into process control.

This research confirmed that concentration is an important factor influencing runaway reaction, as suggested by previous researchers[9]. However, this effect is not uniformly distributed over the wide concentration range. The two patterns are divided in two ranges at the critical point of 40 wt%. This division of concentration range is supported by dominant decomposition reaction pathway postulated in this research.

CHAPTER VI

CONCLUSION AND RECOMMENDATIONS FOR FUTURE WORK

Because of the hazardous properties and wide use of CHP in the chemical industry, there is an urgent need to evaluate its reactivity hazards and apply the results for the prevention of runaway reaction as well as in the design of protection equipment. However, through traditional method of calorimetry test, it is difficult to get a fundamental understanding of the runaway reaction mechanism and perform effective analysis of experimental result. In this research, a systematic approach was utilized to carry out the research at the microscopic level as well as the macroscopic level. By validating theoretical research using experimental data and by applying theoretical research results into experimental studies, it can be concluded that these two levels are linked and interconnected.

In theoretical research, after the analysis of thermodynamic and kinetic stability on the proposed reaction mechanism, a dominant reaction pathway was postulated. The reaction pathway indicates that methane and acetophenone are the major decomposition products, which agrees with experimental results. The reaction equation also reveals that the rate of gas generation is equal to the rate of CHP consumption. It needs to be noticed that in proposed reaction pathway, the ratio between cumene and CHP is 2:1. Therefore, CHP will not completely follow the proposed reaction pathway if the cumene is insufficient. This postulation can be used for industrial application, as well as provide a theoretical basis for experimental research.

In experimental research, the effect of CHP concentration was investigated systematically. The concentration of 40 wt% was proven to be a critical point for almost all important parameters of runaway reactions according to experimental results. For runaway reaction parameters such as maximum temperature, maximum temperature increase, maximum self-heat rate and maximum pressure rate, it was found that concentration factor is more effective in low concentration range (< 40%). But for parameters of maximum pressure, maximum pressure increase, the concentration is more effective in higher concentration range (> 40 wt%). This conclusion agrees with the stoichiometry of the dominant reaction pathway because the mole ratio between cumene and CHP in 40wt% solution is approximate 2: 1. So, in the CHP solution with concentration higher than 40 wt%, part of the CHP follows some unknown reaction pathways, which might be less exothermic and generate more gas.

This result is important for safety issues of CHP. In processes with great variance of CHP concentration, the parameter of pressure for runaway reactions should be emphasized in high concentration range because of its considerable change over concentration. In low concentration range, more attention should be paid to temperature, self-heat rate and pressure rate, as these parameters change greatly over concentration. In addition, heat generation determined in high concentration range cannot be applied to other concentrations because of different reaction pathways involved in decomposition reaction.

Further work is needed to validate the proposed reaction pathway in a quantitative way. Calorimetry test using advanced calorimeter such as APTAC will be used to validate the stoichiometry of the postulated reaction pathway using non-condensable pressure. Also, theoretical calculations using more advanced quantum chemistry method like G2 will be utilized simultaneously to calculate the enthalpy change of recommended reaction pathway. The calculation result will be corrected by the term of heat of evaporation. This calibrated enthalpy change will be compared with empirical data to validate the dominant reaction pathway.

As the involvement of other reaction pathways in decomposition reaction of CHP solution above the concentration of 40 wt%, it is necessary to identify these reaction pathways utilizing quantum chemistry method. The identification of the unknown reaction pathways will get a better understanding of the runaway reaction. It will also provide the basis for further experimental research as well as kinetic modeling.

Compared to calorimeter test method, kinetic modeling is a relatively inexpensive tool to predict and simulate runaway reactions. However, until now, models built can only simulate the runaway reaction in a fixed concentration. Considering the fact that the parameter of concentration varies greatly in many processes, a model will be greatly valuable if it is able to simulate the runaway reaction in different concentrations.

Therefore, following the completion of theoretical research on the reaction mechanism, a kinetic model is planned to be built for the prediction of runaway reactions.

REFERENCES

1. CSB database. In U.S Chemical Safety and Hazard Investigation Board: 2003.

2. Zeiger, E.; Tice, R.; Brevard, B., Cumene hydroperoxide. *Review of Toxicological Literature* **1998,** *80*, 15-9.

3. Cumene Hydroperoxide. http://cameochemicals.noaa.gov/ (Accessed on February, 2008)

4. Code for the Storage of Organic Peroxide Formulations; NFPA 43B. In National Fire Protection Association: Quincy, MA, 1986.

5. Cumene Hydroperoxide. http://www.ilo.org/global/lang--en/index.htm (Accessed on February, 2008)

6. Hou, H. Y.; Duh, Y. S.; Lin, W. H.; Shu, C. M., Reactive incompatibility of cumene hydroperoxide mixedwith alkaline solutions. *Journal of Thermal Analysis and Calorimetry* **2006,** *85*, (1), 145-150.

7. Wang, Y. W.; Shu, C. M.; Duh, Y. S.; Kao, C. S., Thermal runaway hazards of cumene hydroperoxide with contaminants. *Ind. Eng. Chem. Res* **2001,** *4*, 1125-1132.

8. Arendt, J. S.; Casada, M. L.; Rooney, J. J., Reliability and hazards analysis of a cumene hydroperoxide plant. *Plant/Operations Progress* **1986,** *5*, (2), 97-102.

9. Duh, Y. S.; Kao, C. S.; Lee, C.; Yu, S. W., Runaway hazard assessment of cumene hydroperoxide from the cumene oxidation process. *Trans IChemE* **1997,** *75*, (Part B), 73-80.

10. Duh, Y. S.; Kao, C. S.; Hwang, H. H.; Lee, W. W. L., Thermal decomposition kinetics of cumene hydroperoxide. *Trans IChemE* **1998,** *76*, (Part B), 271-276.

11. Chen, K.-Y.; Wu, S.-H.; Wang, Y.-W.; Shu, C.-M., Runaway reaction and thermal hazards simulation of cumene hydroperoxide by DSC. *Journal of Loss Prevention in the Process Industries* **2008,** *21*, (1), 101-109.

12. Kletz, T. A., Fires and explosions of hydrocarbon oxidation plants. *Plant/Operations Progress* **1988,** *7*, (4), 226-230.

13. Mahoney, D.; Consultants, M. P., *Large Property Damage Losses in the Hydrocarbon-chemical Industries: A Thirty-year Review.* M & M Protection Consultants: Chicago, 1993.

14. Recommendations on the Transport of Dangerous Goods, Tests and Criterion, 1st ed. In United Nations: Geneva, Switzerland, 1986; pp 168-189.

15. Recommendations on the Transport of Dangerous Goods, 6th ed. In United Nations: Geneva, Switzerland, 1989; pp 263-275.

16. Leung, J. C.; Creed, M. J.; Fisher, H. G., Round-robin "Vent sizing package" results *Int. Symp. Runaway React* **1989**, 264-280.

17. Kharasch, M. S.; Fono, A.; Nudenberg, W., The chemistry of hydroperoxides. VI. The thermal decomposition of a-cumyl hydroperoxide. *Journal of Organic Chemistry* **1951**, *16*, (1), 113 - 127.

18. Stannett, V.; Mesrobian, R. B., The kinetics of the decomposition of tertiary hydroperoxides in solvents. *J. Am. Chem. Soc.* **1950,** *72*, (9), 4125-4130.

19. Hou, H. Y.; Shu, C. M.; Duh, Y. S., Exothermic decomposition of cumene hydroperoxide at low temperature conditions. *AIChE Journal* **2001,** *47*, (8), 1893-1896.

20. Luo, K.-M.; Chang, J.-G.; Lin, S.-H.; Chang, C.-T.; Yeh, T.-F.; Hu, K.-H.; Kao, C.-S., The criterion of critical runaway and stable temperatures in cumene hydroperoxide reaction. *Journal of Loss Prevention in the Process Industries* **2001,** *14*, (3), 229-239.

21. Tseng, J.-M.; Chang, Y.-Y.; Su, T.-S.; Shu, C.-M., Study of thermal decomposition of methyl ethyl ketone peroxide using DSC and simulation. *Journal of Hazardous Materials* **2007,** *142*, (3), 765-770.

22. Kossoy, A.; Hofelich, T., Methodology and software for assessing reactivity ratings of chemical systems. *Process Safety Progress* **2003,** *22*, (4), 235-240.

23. Kossoy, A.; Benin, A.; Akhmetshin, Y., An advanced approach to reactivity rating. *Journal of Hazardous Materials* **2005,** *118*, (1-3), 9-17.

24. Foresman, J. B.; Frisch, A. E., *Exploring chemistry with electronic structure methods*; Gaussian: Pittsburgh, 1996.

25. Petersson, G. A.; Bennett, A.; Tensfeldt, T. G.; Al-Laham, M. A.; Shirley, W. A.; Mantzaris, J., A complete basis set model chemistry. I. The total energies of closed-shell atoms and hydrides of the first-row elements. *Journal of Chemical physics* **1988**, *89*, (4), 2193-2218.

26. Petersson, G. A.; Al-Laham, M. A., A complete basis set model chemistry. II, Open-shell systems and the total energies of the first-row toams. *Journal of Chemical* Physics **1991**, *94*, (9), 6081-6090.

27. Jursic, B. S., Complete basis set ab initio study of the CH insertion reaction with water, ammonia, and hydrogen fluoride. *J. Phys. Chem. A* **1998,** *102*, (46), 9255-9260.

28. Joseph, W. O.; Petersson, G. A.; J. A. Montgomery, Jr., A complete basis set model chemistry. V. Extensions to six or more heavy atoms. Journal of Chemical Physics, **1996**, *104*, (7), 2598-2619.

29. Benassi, R., A proposed modification of CBS-4M model chemistry for application to molecules of increasing molecular size. *Theoretical Chemistry Accounts* **2001,** *106*, (4), 259-263.

30. Frisch, M. J.; Trucks, G. W.; Schlegel, H. B.; Scuseria, G. E.; Robb, M. A.; Cheeseman, J. R.; Montgomery Jr, J. A.; Vreven, T.; Kudin, K. N.; Burant, J. C., GAUSSIAN 03, Gaussian. *Inc., Pittsburgh, PA* 2003.

31. Bruneton, C.; Hoff, C.; Barton, P. I., Computer aided identification of chemical reaction hazards. *Computers & Chemical Engineering* **1997,** *21*, (Supplement 1), S311-S317.

32. Ludwig, E. E., *Applied Process Design for Chemical and Petrochemical Plants*. Gulf Professional Publishing: New York, 2001.

33. Masel, R. I., *Chemical Kinetics and Catalysis*. John Wiley and Sons: New York: 2001.

34. Aldeeb, A. A. Systematic approach for chemical reactivity evaluation, PhD dissertation, Texas A&M University, College Station, 2003.

35. Fauske, H. K., The reactive system screening tool (RSST): An easy, inexpensive approach to the DIERS procedure. *Process Safety Progress, Vol. 17, No. 3*, **1998**, 191.

36. Levin, M. E.; Gonzales, N. O.; Zimmerman, L. W.; Yang, J., Kinetics of acid-catalyzed cleavage of cumene hydroperoxide. *Journal of Hazardous Materials* **2006,** *130*, (1-2), 88-106.

37. Suppes, G. J.; McHugh, M. A., Solvent and catalytic metal effects on the decomposition of cumene hydroperoxide. *Industrial & Engineering Chemistry Research* **1989,** *28*, (8), 1146-1152.

38. Wei, C.; Rogers, W. J.; Mannan, M. S., Application of runaway reaction mechanism generation to predict and control reactive hazards. *Computers and Chemical Engineering* **2007,** *31*, (3), 121-126.

VITA

Name: Yuan Lu

Address: Room 420, Jack E Brown Building, 3122 TAMU, Texas A&M University, College Station, TX 77843

Email Address: yuan.lu@chemail.tamu.edu

Education: B.S., Biochemical Engineering, East China University of Science and Technology, 2003

M.S., Fermentation Engineering, East China University of Science and Technology, 2006